Available online at www.sciencedirect.com
ScienceDirect
International Journal of Heat and Mass Transfer 50 (2007) 1368–1387
International Journal of HEAT and MASS TRANSFER
www.elsevier.com/locate/ijhmt

Coagulation kernel of particles in a turbulent gas flow

I.V. Derevich *

Department of Thermodynamics and Heat Transfer, Moscow State University of Environmental Engineering, 21/4 Staraya Basmannaya Street, 107884 Moscow, Russia

Received 23 August 2006; received in revised form 8 September 2006
Available online 28 November 2006

Abstract

On the base of modern probability density functions approach turbulent coagulation of particles in gravitational field is investigated. Spectral presentation of second velocity moments of gas phase is used for calculation of intensity of particles relative chaotic motion. Closed diffusion equation for two-particle distribution in space is obtained. Boundary condition taking into account coefficients of new particle formation and momentum restitution during two particles collision is found. Formula for calculation of turbulent coagulation kernel of particles in gravity field is gain. Influence of cloud turbulence and turbulence in a pipe flow on intensity of droplets coagulation is studied. Strong effects of relative turbulent diffusion between droplets, droplets inertia and droplets gravitational settling on intensity of coagulation are found out. Connection between internal structure of turbulence type and coagulation rate is illustrated. Obtained results are right for polydisperse additions in turbulent flows.

1. Introduction

Particles or droplets coagulation in turbulent flows is realized in many industrial technologies and atmospheric phenomenon. Today solution of series of environmental problems demands the investigation of coagulation process of droplets in atmospheric clouds. Mechanisms which control process of droplets coagulation in turbulent atmosphere are very complex. Experimental researches of this process are rather inconvenient and modern methods of studying are based on theoretical investigations. Now are most popular theoretical tools are based on direct numerical simulation (DNS) of turbulent flow with addition a small amount of dispersed phase. Now in the absence of enough trustworthy experimental data about droplets coagulation in atmosphere DNS method can be considered as an image of real experiment.

As a result of analysis of DNS data was revealed that droplets are not uniformly distributed in the turbulent flow. In statistically stationary and homogeneous turbulence are formed fractal structures with preferential concentration of droplets. The results of DNS data about particles collisions and origin of area of increased concentration of particles are collected for example in [1–9]. It was established that effect of preferential concentration is observed for particles dynamic relaxation times are about turbulent Kolmogorov time micro scale. For more inertial particles with relaxation times of order integral time scale of turbulence effect of particles clustering in localized areas of the flow disappears. In [1–9] the collision rate of particles is calculated on the base of averaged relative velocity at the moment of time in which two particles contact with each other. In [7] DNS method is applied to investigation of collision of hydrodynamically interacting particles.

Theoretical methods based on DNS use Lagrange description of a dispersed phase. Lagrange description demands numerical simulation of many thousands particles trajectories with subsequent their averaging. A reliable DNS of turbulent two phase flow is developed for statistically stationary and homogeneous turbulent flow without mass forces working on colliding particles. Including additional factors, for example, gravitational settling of

* Tel./fax: +7 95 362 5590.
E-mail address: nchmt@iht.mpei.ac.ru

0017-9310/$ - see front matter © 2006 Elsevier Ltd. All rights reserved.
doi:10.1016/j.ijheatmasstransfer.2006.09.003

Nomenclature

a_α	radius of αth particle
$B(x,y)$	beta function
C_K	Kolmogorov constant
$D_{\alpha,ik}$	coefficient of turbulent diffusion of αth particles
$D_{\alpha\beta,ik}$	coefficient of turbulent relative diffusion between two particles
D^0	coefficient of turbulent diffusion of inertia less particles
d_α	diameters of αth particle
E_{ij}	correlation of carrier phase velocity fluctuation
$f_\alpha, f_{\alpha\|\beta}$	unconditional and conditional response functions
G	probability density functions of particles displacement
$J_{\alpha\beta}$	flux of βth particles on the surface of αth particle
$K_{\alpha\beta}$	coagulation kernel
$\mathbf{k}$	wave vector in the spectral presentation of velocity correlations
L_E	Euler integral space scale
$N_{\alpha\beta}$	distribution function of particles of two types in space
Re_λ	Reynolds number calculated on Taylor micro scale
T_E	Euler integral temporary scale
$\mathbf{u}$	velocity fluctuations of fluid phase
$\mathbf{V}_\alpha^{(p)}$	actual velocity of the αth particle
$\mathbf{v}_\alpha^{(p)}$	velocity fluctuations of αth particle
$\mathbf{v}_\alpha$	Euler velocity fluctuations of αth particles
$\mathbf{X}_\alpha^{(p)}$	Lagrange position of αth particle
$\mathbf{x}_\alpha$	Euler position of αth particle
$\mathbf{Y}_{\alpha\beta}, \mathbf{y}_{\alpha\beta}$	relative distances between two particles
$\langle \mathbf{W}_\alpha \rangle$	averaged velocity of αth particle due to mass force
$\langle \mathbf{W}_{\alpha\beta} \rangle$	averaged relative velocity between two particles
$\mathbf{w}_{\alpha\beta}$	turbulent relative velocity between two particles

Greek symbols

γ_α	non-dimensional relative velocity of αth particle
Δ	dispersion of particles due to turbulence
$\delta(\mathbf{x})$	three-dimensional Dirac delta-function
ε	turbulent dissipation rate
η_K	Kolmogorov space micro scale
λ	Taylor micro scale
μ	coefficient of momentum restitution after particles collisions
ν	kinematic viscosity of a gas
$\rho_{\alpha\beta}$	coefficient of two particles velocity correlation
σ	average square of particles turbulent velocity
τ_α	dynamic relaxation time of αth particle
τ_K	Kolmogorov temporary micro scale
Φ	probability density function of particles velocity fluctuations
χ	probability of formation new particle as a result of particles collision
Ω_α	parameter of inertia of αth particle
ω_k	mean frequency of velocity fluctuations in eddies with wave vector k

Subscripts

α,β	particles αth and βth types
$\langle\,\rangle$	denotes result of averaging over an ensemble of turbulent realizations

particles, polydisperse of particles leads to essential complication of calculation algorithm and crucial increasing time of numerical simulation. Under these circumstances a number of effects remain unexplored. Main effects include, for example, influence of particles sedimentation velocities on tendency of preferential concentration and coagulation rate, influence of relative turbulent diffusion on particles coagulation, dependence of averaged turbulent relative velocity of particles from their gravitational settling and distance between particles. Therefore results of numerical investigation of coagulation process in a cloud conditions, for example, [10] is questionable. Also rather complex for DNS is investigation of polydisperse composition of particles on their coagulation.

Another way of studying of characteristics of particles in turbulence is based on Euler description. In this approach dispersed phase are treated as continuous media. At comparison of expenses of time request for numerical simulation and complexities of calculation algorithm in DNS the method based on Euler description appears much more economic than DNS. As a result of Euler description we obtain the system of balance equations for first and second moments of dispersed phase fluctuations. Advantages of this approach consist from not only sufficient reduction of computational time, but also in opportunity of inclusion of various complicating factors at studying turbulent flow with colliding particles. Really in Euler description always remain questions about legitimacy of assumption used for closing the system of equations. Nevertheless modeling of turbulent motion of particles as continuous phase is very attractive. Reasonable combination of Lagrange and Euler approaches for description turbulent motion of particles should lead to understanding the basically lows in complex conditions realized in modern technologies and atmospheric phenomenon.

Essential way to transit from Lagrange description to Euler is based on probability density function (PDF) for various parameters of particles, for example, coordinates, velocities, temperatures and others (see, for reference, [11–13]). Closed equation for PDF gives system of balance

equations for moments of dispersed phase parameters. For example, PDF of two particles distribution in space is describes by diffusion equation. According to type of the equation it is required to build up boundary conditions. Necessary boundary conditions are found at the present work. First condition describes particles which are separated from each other on the sufficiently large distance. Second boundary condition is on the colliding sphere at the moment of particles collision. In the second boundary condition we take into account probability of new particle formation and momentum loss during particles collisions with each other. In the sense of the diffusion equation the rate of particles coagulation is represent as flux of colliding particles on the surface of a set particle considered as a target.

Results of the present work used the main ideas and approaches of our previous article [13]. The main goal of this paper is investigation of influence of relative turbulent diffusion between particles, sedimentation velocities of particles and particles inertia on the rate of coagulation. Brownian motion of particles investigated in our work is negligible small in comparison of intensity of particles turbulence, so main origin of particles chaotic motion is turbulence of carried phase.

The calculation results are compared with available DNS data. Qualitative features in chaotic behavior of particles in various types of turbulence in an atmospheric cloud and in a pipe flows are illustrated. On the base of spectral presentation of correlation of carrier phase velocity fluctuations results of [13] are improved. In this paper, we do not study effect of preferential concentration of particles. Results of present paper are accurate for particles with relaxation times surpassing the Kolmogorov temporary micro scale.

2. Particle response functions

If we consider two points in stationary and isotropic turbulence, we find out, that temporary and space integral scales along line between these points and perpendicular to the line are different (see, for example, [14]). Essential way to include such information in calculations of particles response functions [13] is based on use spectral presentation of second moments of carrier phase velocity fluctuations. Also it is important that spectral approach enables take into account in the calculations detailed information about microstructure of turbulence.

2.1. Unconditional response function

Intensity of particles turbulent motion in equilibrium approach depends on response function [13]

$$\langle v_{\alpha,i} v_{\alpha,j}\rangle = f_\alpha \langle u_i u_j\rangle,$$
$$\langle u_i u_j\rangle f_\alpha = \frac{1}{\tau_\alpha}\int_0^t \mathrm{e}^{-\frac{t-\xi}{\tau_\alpha}} \left\langle u_i(\mathbf{x},t) u_j\left(\mathbf{X}_\alpha^{(\mathrm{p})}(\xi),\xi\right)\right\rangle \mathrm{d}\xi, \tag{1}$$

where τ_α is αth particle dynamic relaxation time; $\mathbf{X}_\alpha^{(\mathrm{p})}(\xi)$ is random particle trajectory, which in the moment of time t is passes through point $\mathbf{x}$, $\mathbf{X}_\alpha^{(\mathrm{p})}(t)=\mathbf{x}$; $\langle v_{\alpha i} v_{\alpha j}\rangle$ is second moment of αth particles velocity fluctuations. Averaging in (1) is carried over the ensembles of turbulent realizations of gas and particles velocity fluctuations. In the sense of Corrsin [15] "independent hypothesis" we rewrite (1) in the spectral form (see Appendix A)

$$\langle u_i u_j\rangle f_\alpha = \frac{1}{\tau_\alpha}\int_0^\infty \mathrm{e}^{-\frac{s}{\tau_\alpha}}\mathrm{d}s \times \int \widehat{E}_{ij}(\mathbf{k},s)\left\langle \exp\left[\mathrm{i}\mathbf{k}\cdot\left(\mathbf{X}_\alpha^{(\mathrm{p})}(t)-\mathbf{X}_\alpha^{(\mathrm{p})}(t-s)\right)\right]\right\rangle \mathrm{d}\mathbf{k}, \tag{2}$$

where $s=t-\xi$; in the exponential term in (2) $\mathrm{i}^2=-1$, i is complex unit; point in exponential term denotes scalar product of two vectors; $\widehat{E}_{ij}(\mathbf{k},s)$ is spectral presentation of two-point two-time correlation of carrier phase velocity fluctuations (see Appendix A).

The response function for particles turbulent energy follows from (2) and has simpler form:

$$\frac{3}{2}\left\langle v_\alpha^2\right\rangle = \frac{1}{2} f_\alpha \langle u_i u_i\rangle = f_\alpha E, \tag{3}$$

where is meant summation on twice repeated index.

The term in the angular brackets in the right-hand side of expression (2) has the form

$$\left\langle \exp\left[\mathrm{i}\mathbf{k}\cdot\left(\mathbf{X}_\alpha^{(\mathrm{p})}(t)-\mathbf{X}_\alpha^{(\mathrm{p})}(t-s)\right)\right]\right\rangle = \left\langle \exp\left[\mathrm{i}\mathbf{k}\cdot\mathbf{Y}_\alpha^{(\mathrm{p})}(s)\right]\right\rangle,$$

where $\mathbf{Y}_\alpha^{(\mathrm{p})}(s)=\mathbf{X}_\alpha^{(\mathrm{p})}(t)-\mathbf{X}_\alpha^{(\mathrm{p})}(t-s)=\int_0^s \mathbf{V}_\alpha^{(\mathrm{p})}(\xi)\,\mathrm{d}\xi$ is random displacement of a particle during interval of time s; $\mathbf{V}_\alpha^{(\mathrm{p})}(\xi)$ is a particle instantaneous velocity.

In the coordinate frame moving with average velocity of carrier phase we separate relative average velocity of particle $\langle \mathbf{W}_\alpha\rangle$ and velocity fluctuation $\mathbf{v}_\alpha^{(\mathrm{p})}$

$$\mathbf{V}_\alpha^{(\mathrm{p})}(\xi) = \langle \mathbf{W}_\alpha\rangle + \mathbf{v}_\alpha^{(\mathrm{p})}(\xi), \quad \left\langle \mathbf{v}_\alpha^{(\mathrm{p})}(\xi)\right\rangle = 0.$$

With the account of above formulas we obtain

$$\left\langle \exp\left[\mathrm{i}\mathbf{k}\cdot\mathbf{Y}_\alpha^{(\mathrm{p})}(s)\right]\right\rangle = \exp(\mathrm{i}\mathbf{k}\cdot\langle\mathbf{W}_\alpha\rangle s)\left\langle \exp\left[\mathrm{i}\mathbf{k}\cdot\int_0^s \mathbf{v}_\alpha^{(\mathrm{p})}(\xi)\,\mathrm{d}\xi\right]\right\rangle = \exp(\mathrm{i}\mathbf{k}\cdot\langle\mathbf{W}_\alpha\rangle s)\left\langle \exp\left[\mathrm{i}\mathbf{k}\cdot\mathbf{y}_\alpha^{(\mathrm{p})}(s)\right]\right\rangle, \tag{4}$$

where $\mathbf{y}_\alpha^{(\mathrm{p})}(s)=\int_0^s \mathbf{v}_\alpha^{(\mathrm{p})}(\xi)\,\mathrm{d}\xi$ is random particle displacement during interval of time s.

The two multipliers in the last term of (4) describe effects due to average velocity slips and due to chaotic motion of particle. Averaged value of multiplier which connected with particle chaotic motion is calculated with the help of PDF of particles displacement $G(\mathbf{y}_\alpha,s)$

$$\left\langle \exp\left[\mathrm{i}\mathbf{k}\cdot\mathbf{y}_\alpha^{(\mathrm{p})}(s)\right]\right\rangle = \int G(\mathbf{y}_\alpha,s)\exp(\mathrm{i}\mathbf{k}\cdot\mathbf{y}_\alpha)\,\mathrm{d}\mathbf{y}_\alpha. \tag{5}$$

We consider particle velocity fluctuations as a statistically stationary Gaussian random process. For particles with dynamic relaxation times of order integral time scale of turbulence DNS data (see, for example, [2]) confirm this

assumption. Being based on the results of the previous paper [13] expression for PDF $G(\mathbf{y}_\alpha,s)$ of particle random displacement it is written as

$$G(\mathbf{y}_\alpha,s)=\frac{1}{\left(2\pi\Delta_\alpha^2(s)\right)^{3/2}}\exp\left(-\frac{\mathbf{y}_\alpha\cdot\mathbf{y}_\alpha}{2\Delta_\alpha^2(s)}\right). \tag{6}$$

Here $\Delta_\alpha^2(s)$ is averaged square of module of particle chaotic displacement due to its inertia

$$\Delta_\alpha^2(s)=\Xi^2\tau_\alpha^2\langle v_\alpha^2\rangle\left[1-\exp\left(-\frac{s}{\tau_\alpha}\right)\right]^2, \tag{7}$$

where multiplier Ξ is defined in Appendix B (formula (B.3)).

In (7) $\langle v_\alpha^2\rangle$ is averaged square of particle velocity fluctuations

$$\langle v_\alpha^2\rangle=f_\alpha u^2,\quad \frac{3}{2}u^2=E,$$

were u is mean turbulent velocity of carrier phase. From formulas (5) and (6) we obtain (see Appendix B, formula (B.6)) closed expression for averaged value in (5)

$$\left\langle\exp\left[\mathrm{i}\mathbf{k}\cdot\mathbf{y}_\alpha^{(\mathrm{p})}(s)\right]\right\rangle=\exp\left[-\frac{k^2\Delta_\alpha^2(s)}{2}\right]. \tag{8}$$

Final expression for response function of particle (1) in spectral form follows from (2), (4), (5) and (8)

$$\langle u_iu_j\rangle f_\alpha=\frac{1}{\tau_\alpha}\int\mathrm{d}\mathbf{k}\int_0^\infty \mathrm{e}^{-\frac{s}{\tau_\alpha}}\widehat{E}_{ij}(\mathbf{k},s)\exp\left[\mathrm{i}\mathbf{k}\cdot\langle\mathbf{W}_\alpha\rangle s-\frac{k^2\Delta_\alpha^2}{2}\right]\mathrm{d}s. \tag{9}$$

Here the value of averaged square of particles random displacement (7) we estimate for $s=T_\mathrm{E}$

$$\Delta_\alpha^2=\Delta_\alpha^2(T_E).$$

As one can see from (7), for low inertial particle $\tau_\alpha\to 0$ there no inertial flight of particle $\Delta_\alpha^2\to 0$. For particle with sufficient inertia $\tau_\alpha\gg T_\mathrm{E}$ the length of averaged particle transfer also aspires to zero as $\Delta_\alpha^2\to u^2T_\mathrm{E}^2(T_\mathrm{E}/\tau_\alpha)$.

The response function for turbulent energy of particles (3) has form simpler than (9)

$$f_\alpha=\frac{1}{E}\int_0^\infty\widehat{E}^0(k)\exp\left(-\frac{k^2\Delta_\alpha^2}{2}\right)\frac{\operatorname{arctg}\left(\frac{k\tau_\alpha\langle W_\alpha\rangle}{1+\omega_k\tau_\alpha}\right)}{k\tau_\alpha\langle W_\alpha\rangle}\mathrm{d}k, \tag{10}$$

where $\langle W_\alpha\rangle$ is module of average relative velocity of αth particle.

From (10) one can see that response function reduced with increasing particles relaxation time and average relative velocity. Dependence of the response function on average velocity is result of the so-called "crossing trajectory effect" [16].

2.2. Conditional response function

Conditional response function has the form [13]

$$f_{\beta|\alpha}(\mathbf{y}_{\alpha\beta})\langle u_iu_j\rangle=\frac{1}{\tau_\beta}\int_0^t\mathrm{e}^{-\frac{t-\xi}{\tau_\beta}}\left\langle u_i(\mathbf{x}_\alpha,t)u_j\left(\mathbf{X}_\beta^{(\mathrm{p})}(\xi),\xi\right)\right\rangle\mathrm{d}\xi, \tag{11}$$

where $\mathbf{y}_{\alpha\beta}=\mathbf{x}_\alpha-\mathbf{x}_\beta$ is relative distance between particles at the moment of time t.

Eq. (11) describes the results of averaging over ensembles of turbulent realization of velocity fluctuations of carrier phase and random trajectories of particles α and β in condition, that at the moment of time t distance between particles will be $\mathbf{y}_{\alpha\beta}$. In spectral presentation of carrier phase velocity fluctuations the expression (11) turns to

$$f_{\beta|\alpha}(\mathbf{y}_{\alpha\beta})\langle u_iu_j\rangle=\frac{1}{\tau_\beta}\int\mathrm{d}\mathbf{k}\int_0^\infty\mathrm{e}^{-\frac{s}{\tau_\beta}}\widehat{E}_{ij}(\mathbf{k},s)\left\langle\exp\left[\mathrm{i}\mathbf{k}\cdot\left(\mathbf{X}_\alpha^{(\mathrm{p})}(t)-\mathbf{X}_\beta^{(\mathrm{p})}(\xi)\right)\right]\right\rangle\mathrm{d}s, \tag{12}$$

where $s=t-\xi$.

The difference in random trajectories of two particles in (12) can be submitted in the equivalent form

$$\begin{aligned}\mathbf{X}_\alpha^{(\mathrm{p})}(t)-\mathbf{X}_\beta^{(\mathrm{p})}(\xi)&=\left[\mathbf{X}_\alpha^{(\mathrm{p})}(t)-\mathbf{X}_\alpha^{(\mathrm{p})}(\xi)\right]+\left[\mathbf{X}_\alpha^{(\mathrm{p})}(\xi)-\mathbf{X}_\beta^{(\mathrm{p})}(\xi)\right]\\&=\mathbf{Y}_\alpha^{(\mathrm{p})}(s)+\mathbf{Y}_{\alpha\beta}^{(\mathrm{p})}(\xi),\\ \mathbf{Y}_{\alpha\beta}^{(\mathrm{p})}(\xi)&=\mathbf{X}_\alpha^{(\mathrm{p})}(\xi)-\mathbf{X}_\beta^{(\mathrm{p})}(\xi),\end{aligned} \tag{13}$$

where $\mathbf{Y}_{\alpha\beta}^{(\mathrm{p})}(\xi)$ is random relative displacement of two particles during interval of time ξ.

Instantaneous relative distance between two particles at an arbitrary moment of time $t^0\leqslant\xi\leqslant t$ is

$$\mathbf{Y}_{\alpha\beta}^{(\mathrm{p})}(\xi)=\langle\mathbf{W}_{\alpha\beta}\rangle\left(\xi-t^0\right)+\mathbf{z}_{\alpha\beta}^{(\mathrm{p})}(\xi)+\mathbf{Y}_{\alpha\beta}^0, \tag{14}$$

where $\langle\mathbf{W}_{\alpha\beta}\rangle=\langle\mathbf{W}_\alpha\rangle-\langle\mathbf{W}_\beta\rangle$ is difference between averaged velocities of particles; t^0 is initial moment of time; $\mathbf{Y}_{\alpha\beta}^0$ is relative distance between particles at the initial moment of time t^0; $\mathbf{z}_{\alpha\beta}^{(\mathrm{p})}(\xi)$ is random component of relative distance, $\left\langle\mathbf{z}_{\alpha\beta}^{(\mathrm{p})}(\xi)\right\rangle=0$.

Relative distance between particles at the moment of time t is exact $\mathbf{y}_{\alpha\beta}$

$$\mathbf{Y}_{\alpha\beta}^{(\mathrm{p})}(t)=\mathbf{y}_{\alpha\beta}=\langle\mathbf{W}_{\alpha\beta}\rangle(t-t^0)+\mathbf{Y}_{\alpha\beta}^0. \tag{15}$$

From Eqs. (14) and (15) follows equation for relative distance between two particles for any moment of time $t^0\leqslant\xi\leqslant t$

$$\mathbf{Y}_{\alpha\beta}^{(\mathrm{p})}(\xi)=\mathbf{y}_{\alpha\beta}-\langle\mathbf{W}_{\alpha\beta}\rangle(t-\xi)+\mathbf{z}_{\alpha\beta}^{(\mathrm{p})}(\xi). \tag{16}$$

After substitution expressions (4), (13) and (16) into expression (12) we find following formula for conditional response function

$$f_{\beta|\alpha}(\mathbf{y}_{\alpha\beta})\langle u_i u_j\rangle = \frac{1}{\tau_\beta}\int \mathrm{d}\mathbf{k}\int_0^\infty \mathrm{e}^{-\frac{s}{\tau_\beta}}\widehat{E}_{ij}(\mathbf{k},s)\exp[\mathrm{i}\mathbf{k}\cdot\langle\mathbf{W}_\alpha\rangle s] \times\left\langle\exp\left[\mathrm{i}\mathbf{k}\cdot\mathbf{y}_\alpha^{(\mathrm{p})}(s)\right]\right\rangle\exp[\mathrm{i}\mathbf{k}\cdot(\mathbf{y}_{\alpha\beta}-\langle\mathbf{W}_{\alpha\beta}\rangle s)] \times\left\langle\exp\left[\mathrm{i}\mathbf{k}\cdot\mathbf{z}_{\alpha\beta}^{(\mathrm{p})}(\xi)\right]\right\rangle\mathrm{d}s. \quad (17)$$

At writing (17) we have split correlation between random motion of αth particle and relative motion between two particles.

We suppose that relative velocity between two particles is Gaussian random process. Under this supposition averaged value of the last multiplier in the right-hand side of (17) is calculated as

$$\left\langle\exp\left[\mathrm{i}\mathbf{k}\cdot\mathbf{z}_{\alpha\beta}^{(\mathrm{p})}(\xi)\right]\right\rangle = \int G(\mathbf{z}_{\alpha\beta},\xi)\exp\left(\mathrm{i}\mathbf{k}\cdot\mathbf{z}_{\alpha\beta}\right)\mathrm{d}\mathbf{z}_{\alpha\beta}. \quad (18)$$

Here $G(\mathbf{z}_{\alpha\beta},\xi)$ presents PDF of random distance between two particles at the moment of time ξ. On the basis of results [13] one can write down

$$G(\mathbf{z}_{\alpha\beta},\xi) = \frac{1}{\left(2\pi\Delta_{\alpha\beta}^2(\xi)\right)^{3/2}}\exp\left(-\frac{\mathbf{z}_{\alpha\beta}\cdot\mathbf{z}_{\alpha\beta}}{2\Delta_{\alpha\beta}^2(\xi)}\right). \quad (19)$$

After substitution (19) into (18) with the help of Appendix B we obtain

$$\left\langle\exp\left[\mathrm{i}\mathbf{k}\cdot\mathbf{z}_{\alpha\beta}^{(\mathrm{p})}(\xi)\right]\right\rangle = \exp\left[-\frac{k^2\Delta_{\alpha\beta}^2(\xi)}{2}\right]. \quad (20)$$

Nonzero value of sub integral function in (17) is located in the interval of time $t - T_\mathrm{E} \leqslant \xi \leqslant t$. In that case for moments of time $(\xi - t^0) \gg T_\mathrm{E}$, τ_α, τ_β averaged square of random relative distance between two particles is approximated as (see [13])

$$\Delta_{\alpha\beta}^2 = \Xi^2\left(\tau_\alpha^2\left\langle v_\alpha^2\right\rangle + \tau_\beta^2\left\langle v_\beta^2\right\rangle - 2\rho_{\alpha\beta}\tau_\alpha\tau_\beta\sqrt{\left\langle v_\alpha^2\right\rangle\left\langle v_\beta^2\right\rangle}\right),$$

where $\rho_{\alpha\beta}$ is correlation coefficient between random velocities of two particles.

Value of inertial displacement of particles $\Delta_{\alpha\beta}^2$ grows with increasing particles relaxation times. For inertial particles $\tau_\alpha, \tau_\beta \gg T_\mathrm{E}$ square of relative distance between particles tends to $\Delta_{\alpha\beta}^2 \approx \Xi^2(u^2 T_\mathrm{E})(\tau_\alpha + \tau_\beta)$. Correlation coefficient $\rho_{\alpha\beta}$ is connected with unconditional and conditional response functions (see [13])

$$\rho_{\alpha\beta} = \frac{\Omega_\beta f_{\beta|\alpha} + \Omega_\alpha f_{\alpha|\beta}}{(f_\alpha f_\beta)(\Omega_\alpha + \Omega_\beta)}, \quad (21)$$

where $\Omega_\alpha = \tau_\alpha / T_\mathrm{E}$ is parameter of particles inertia.

From expressions (8), (17) and (20) follows closed formula for conditional response function in spectral presentation

$$f_{\beta|\alpha}(\mathbf{y}_{\alpha\beta})\langle u_i u_j\rangle = \frac{1}{\tau_\beta}\int \mathrm{d}\mathbf{k}\int_0^\infty \mathrm{e}^{-\frac{s}{\tau_\beta}}\widehat{E}_{ij}(\mathbf{k},s)\exp[\mathrm{i}\mathbf{k}\cdot(\langle\mathbf{W}_\beta\rangle s + \mathbf{y}_{\alpha\beta})] \times\exp\left[-\frac{k^2}{2}\left(\Delta_\alpha^2 + \Delta_{\alpha\beta}^2\right)\right]\mathrm{d}s. \quad (22)$$

Simpler expression for conditional response function follows from (22) for $\mathbf{y}_{\alpha\beta} = 0$ after summation over $i = j$

$$f_{\beta\alpha} = \frac{1}{E}\int_0^\infty \widehat{E}^0(k)\exp\left[-\frac{k^2}{2}\left(\Delta_\alpha^2 + \Delta_{\alpha\beta}^2\right)\right]\frac{\mathrm{arctg}\left(\frac{k\tau_\beta\langle W_\beta\rangle}{1+\omega_k\tau_\beta}\right)}{k\tau_\beta\langle W_\beta\rangle}\mathrm{d}k. \quad (23)$$

From (23) it is possible to notice, that conditional response function decrease with increasing average relative velocity and relaxation times of particles αth or βth types.

Square of relative chaotic velocity between particles for isotropic turbulent flow has the form

$$\left\langle w_{\alpha\beta}^2\right\rangle = \langle(v_\alpha - v_\beta)^2\rangle = \left\langle v_\alpha^2\right\rangle + \left\langle v_\beta^2\right\rangle - 2\rho_{\alpha\beta}\sqrt{\left\langle v_\alpha^2\right\rangle\left\langle v_\beta^2\right\rangle}. \quad (24)$$

Averaged module of relative velocity between particles is calculated in accordance of Appendix B

$$\langle|w_{\alpha\beta}|\rangle = \Xi\sqrt{\left\langle w_{\alpha\beta}^2\right\rangle}. \quad (25)$$

3. Turbulent diffusion coefficients of particles

Turbulent relative diffusion coefficient of two particles has been definite in [13]

$$D_{\alpha\beta,ij}(\mathbf{y}_{\alpha\beta}) = \int_0^t\left\{\left\langle u_i(\mathbf{x}_\alpha,t)\left[u_j\left(\mathbf{X}_\alpha^{(\mathrm{p})}(\xi),\xi\right) - u_j\left(\mathbf{X}_\beta^{(\mathrm{p})}(\xi),\xi\right)\right]\right\rangle + \left\langle u_i(\mathbf{x}_\beta,t)\left[u_j\left(\mathbf{X}_\beta^{(\mathrm{p})}(\xi),\xi\right) - u_j\left(\mathbf{X}_\alpha^{(\mathrm{p})}(\xi),\xi\right)\right]\right\rangle\right\}\mathrm{d}\xi. \quad (26)$$

From (26) it is follows that relative turbulent diffusion of particles is function of distance between particles. The coefficient of relative turbulent diffusion can be submitted as a combination of coefficients of turbulent diffusions of particles αth and βth types and additional term, which depends on particles correlation

$$D_{\alpha\beta,ij}(\mathbf{y}_{\alpha\beta}) = D_{\alpha,ij} + D_{\beta,ij} - B_{\alpha\beta,ij}(\mathbf{y}_{\alpha\beta}), \quad (27)$$

where $D_{\alpha,ij}$, $D_{\beta,ij}$ are usual coefficients of turbulent diffusion of particles; $B_{\alpha\beta\cdot ij}$ is additional term caused by correlation motion of various particles.

Coefficient of turbulent diffusion αth particles has the form

$$D_{\alpha,ij} = \int_0^t\left\langle u_i(\mathbf{x}_\alpha,t)u_j\left(\mathbf{X}_\alpha^{(\mathrm{p})}(\xi),\xi\right)\right\rangle\mathrm{d}\xi.$$

In spectral presentation of fluid velocity correlation the above expression becomes as (see, for example (9))

$$D_{\alpha,ij} = \int\mathrm{d}\mathbf{k}\int_0^t\widehat{E}_{ij}(\mathbf{k},s)\exp\left[\mathrm{i}\mathbf{k}\cdot\langle\mathbf{W}_\alpha\rangle s - \frac{k^2\Delta_\alpha^2(s)}{2}\right]\mathrm{d}s. \quad (28)$$

By analogy of (22) we find the presentation of additional term in expression (27)

$$B_{\alpha\beta,ij}(\mathbf{y}_{\alpha\beta}) = \int \mathrm{d}\mathbf{k}\exp(\mathrm{i}\mathbf{k}\cdot\mathbf{y}_{\alpha\beta})\int_0^t \widehat{E}_{ij}(\mathbf{k},s)\exp\left(-\frac{k^2\Delta_{\alpha\beta}^2}{2}\right) \times\left[\exp\left(\mathrm{i}\mathbf{k}\cdot\langle\mathbf{W}_\beta\rangle s-\frac{k^2\Delta_\alpha^2}{2}\right)+\exp\left(\mathrm{i}\mathbf{k}\cdot\langle\mathbf{W}_\alpha\rangle s-\frac{k^2\Delta_\beta^2}{2}\right)\right]\mathrm{d}s. \tag{29}$$

From expressions (28) and (29) one can conclude that increasing of average relative velocities of particles reduced coefficients of turbulent diffusions. Additional term connected with particles correlation motion also diminishes with grows of relative distance between particles $\mathbf{y}_{\alpha\beta}$.

For simplicity of the further calculation we will examine the mean values of turbulent diffusions

$$D_\alpha = \frac{1}{3}D_{\alpha,ii},\quad D_{\alpha\beta}(\mathbf{y}_{\alpha\beta}) = \frac{1}{3}D_{\alpha\beta,ii}(\mathbf{y}_{\alpha\beta}).$$

In spectral presentation of turbulent energy the expression for mean coefficient of turbulent diffusion can be calculated by analogy of (10)

$$D_\alpha = \frac{2}{3}\int_0^\infty \frac{\widehat{E}^0(k)}{\omega_k}\exp\left(-\frac{k^2\Delta_\alpha^2}{2}\right)\frac{\mathrm{arctg}(k\langle W_\alpha\rangle/\omega_k)}{k\langle W_\alpha\rangle/\omega_k}\,\mathrm{d}k. \tag{30}$$

From (30) follows that grows of average relative velocity of particles reduced coefficient of turbulent diffusion ("crossing trajectories effect" [16]).

For inertia loss particles without average relative velocity expression (30) turns out to formula for turbulent diffusion of passive substance

$$D^0 = \frac{2}{3}\int_0^\infty \frac{\widehat{E}^0(k)}{\omega_k}\,\mathrm{d}k.$$

Expression for coefficient of relative turbulent diffusion of particles we write down for $\mathbf{y}_{\alpha\beta}=0$ in (29)

$$D_{\alpha\beta} = D_\alpha + D_\beta - B_{\alpha\beta},$$
$$B_{\alpha\beta} = \frac{2}{3}\int_0^\infty \frac{\widehat{E}^0(k)}{\omega_k}\exp\left(-\frac{k^2\Delta_{\alpha\beta}^2}{2}\right)\left[\exp\left(-\frac{k^2\Delta_\beta^2}{2}\right)\frac{\mathrm{arctg}(k\langle W_\alpha\rangle/\omega_k)}{k\langle W_\alpha\rangle/\omega_k} + \exp\left(-\frac{k^2\Delta_\alpha^2}{2}\right)\frac{\mathrm{arctg}(k\langle W_\beta\rangle/\omega_k)}{k\langle W_\beta\rangle/\omega_k}\right]\mathrm{d}k.$$

For inertial particles $\tau_\alpha, \tau_\beta \gg T_\mathrm{E}$ or for sufficient average relative velocities of particles $k\langle W_\beta\rangle/\omega_k \gg 1$ the additional term $B_{\alpha\beta}$ aspires to zero and coefficient of relative turbulent diffusion becomes a sum of usual coefficients of turbulent diffusion of particles.

4. Coagulation kernel

4.1. Analysis of equation for distribution of two particles in space

Particles distribution at two points in space is described by function [13]

$$\langle N_{\alpha\beta}(\mathbf{x}_\alpha,\mathbf{x}_\beta,t)\rangle = \left\langle\delta\left(\mathbf{x}_\alpha-\mathbf{X}_\alpha^{(\mathrm{p})}(t)\right)\delta\left(\mathbf{x}_\beta-\mathbf{X}_\beta^{(\mathrm{p})}(t)\right)\right\rangle. \tag{31}$$

In (31) it is possible to allocate mean $\mathbf{x}_{\alpha\beta}$ and relative $\mathbf{y}_{\alpha\beta}$ variables

$$\langle N_{\alpha\beta}(\mathbf{x}_{\alpha\beta},\mathbf{y}_{\alpha\beta},t)\rangle = \left\langle\delta\left\{\mathbf{x}_{\alpha\beta}-\left[\mathbf{X}_\alpha^{(\mathrm{p})}(t)+\mathbf{X}_\beta^{(\mathrm{p})}(t)\right]/2\right\} \times\delta\left\{\mathbf{y}_{\alpha\beta}-\left[\mathbf{X}_\alpha^{(\mathrm{p})}(t)-\mathbf{X}_\beta^{(\mathrm{p})}(t)\right]\right\}\right\rangle,$$

where $\mathbf{x}_{\alpha\beta}=(\mathbf{x}_\alpha+\mathbf{x}_\beta)/2$, $\mathbf{y}_{\alpha\beta}=\mathbf{x}_\alpha-\mathbf{x}_\beta$ are mean and relative variables accordingly.

Scale of change the two particles distribution on mean variable $\mathbf{x}_{\alpha\beta}$ sufficiently exceeds scale of change along the relative variable $\mathbf{y}_{\alpha\beta}$. In the previous paper [13] on the base of PDF approach was obtained equation for two particles distribution in relative variable. We consider this equation without variation of second moment of two particles velocities fluctuations

$$\frac{\partial\langle N_{\alpha\beta}\rangle}{\partial t}+\frac{\partial}{\partial y_{\alpha\beta,i}}\left(\langle W_{\alpha\beta,i}\rangle\langle N_{\alpha\beta}\rangle - D_{\alpha\beta,ij}\frac{\partial\langle N_{\alpha\beta}\rangle}{\partial y_{\alpha\beta,j}}\right)=0. \tag{32}$$

Eq. (32) determines vector of averaged relative velocity of dispersed phase $\langle\widetilde{\mathbf{W}}_{\alpha\beta}\rangle$

$$\frac{\partial\langle N_{\alpha\beta}\rangle}{\partial t}+\frac{\partial}{\partial y_{\alpha\beta,i}}\left(\left\langle\widetilde{W}_{\alpha\beta,i}\right\rangle\langle N_{\alpha\beta}\rangle\right)=0,$$
$$\left\langle\widetilde{W}_{\alpha\beta,i}\right\rangle = \langle W_{\alpha\beta,i}\rangle - D_{\alpha\beta,il}\frac{\partial\ln\langle N_{\alpha\beta}\rangle}{\partial y_{\alpha\beta,j}}. \tag{33}$$

We examine flux $\mathbf{J}_{\alpha\beta}$ of βth type particles on surface of αth type particle, which is considered as a target (see Fig. 1)

$$\mathbf{J}_{\alpha\beta}\left\langle N_{\alpha\beta}^0\right\rangle = \left(\left\langle\widetilde{\mathbf{W}}_{\alpha\beta}\right\rangle\langle N_{\alpha\beta}\rangle\right)\Big|_{S_{\alpha\beta}}, \tag{34}$$

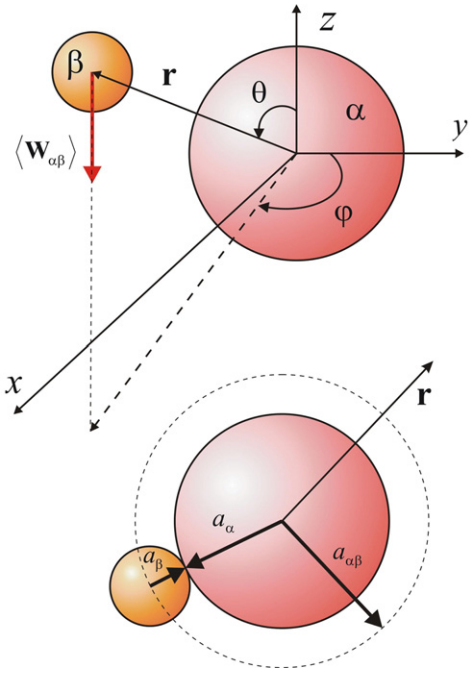

Fig. 1. The sketch of particles collisions, when αth particle considered as a target.

where $\langle N^0_{\alpha\beta}\rangle$ is distribution of particles, when coordinate $\mathbf{x}_\beta$ is positioned sufficiently far from point $\mathbf{x}_\alpha$; index $S_{\alpha\beta}$ in the right-hand side of (34) denotes that function is calculated on the effective colliding sphere with radius $a_{\alpha\beta}$ (see Fig. 1).

Collision of particles with each other can lead to formation of new particle, or to disintegration of particles. Also after collision particles may loss momentum of their relative motion. These processes control distribution of dispersed impurity concentration in space. The description of various behaviors of particles after collision is incorporated in boundary condition at the colliding sphere.

4.2. Boundary condition for colliding particles

Boundary condition for distribution of two particles in space we obtain in the frame of statistical approach [11]. Actual relative velocity in dispersed phase consist from averaged (3) and fluctuating parts

$$\widetilde{\mathbf{W}}_{\alpha\beta} = \left\langle \widetilde{\mathbf{W}}_{\alpha\beta} \right\rangle + \mathbf{w}_{\alpha\beta}, \quad \langle \mathbf{w}_{\alpha\beta} \rangle = 0.$$

Relative velocity may be presented as a sum of velocities in radial $\widetilde{\mathbf{W}}_n$ and tangential $\widetilde{\mathbf{W}}_t$ directions by following formulas

$$\widetilde{\mathbf{W}}_n = \mathbf{n}\left(\mathbf{n}\cdot\widetilde{\mathbf{W}}_{\alpha\beta}\right), \quad \widetilde{\mathbf{W}}_t = \widetilde{\mathbf{W}}_{\alpha\beta} - \mathbf{n}\left(\mathbf{n}\cdot\widetilde{\mathbf{W}}_{\alpha\beta}\right), \quad \mathbf{n} = \mathbf{r}/r.$$

Method using in treatment boundary condition at the colliding sphere is similar to the method used in the kinetic theory of gaseous [17].

Collided particles can form new particle with probability $1-\chi$, or remain separate particles with probability χ. We investigate only coagulation of droplets. As a rule droplets breakup is results of two reasons. First reason connected with sufficiently large difference in velocities between colliding droplets. Second reason is significant viscous stresses on the droplets surface due to relative velocities between droplets and surrounding fluid. These both reasons are realized, for example, in nonequilibrium turbulent flows such as turbulent jets, initial stage of pipe flow, or turbulent flow in various mixers. In clouds turbulence or in turbulence at stabilized flow in a pipe relative velocities between droplets is not so significant to lead to droplets breakup.

During inelastic collision particles lose the momentum of their relative motion. The radial relative velocity of reflected particles changes sign. Direction of tangential relative velocity of reflected particles does not vary. With these assumptions PDF of reflected particles $\Phi_+(\mathbf{W}''_{\alpha\beta})$ is connected with PDF of colliding particles $\Phi_-(\mathbf{W}'_{\alpha\beta})$ as

$$W''_n\Phi_+(W''_n,\mathbf{W}''_t) = -\chi\int_{-\infty}^{0} \mathrm{d}W'_n \int W'_n\Phi_-(W'_n,\mathbf{W}'_t)\delta(W'_n\mu_n + W''_r)\delta(\mathbf{W}'_t\mu_t - \mathbf{W}''_t)\,\mathrm{d}\mathbf{W}'_t, \tag{35}$$

where one and two primes denote the velocities of particles before and after collision; μ_n, μ_t are coefficients of momentum restitution in radial and tangential directions.

After integration (35) we obtain following presentation for PDF of reflected particles

$$\Phi_+(W''_n,\mathbf{W}''_t) = \frac{\chi}{\mu_n^2\mu_t}\Phi_-\left(-\frac{W''_n}{\mu_n},\frac{\mathbf{W}''_t}{\mu_t}\right). \tag{36}$$

In homogeneous approximation the PDF of particles before collision is

$$\Phi_-(W'_n,\mathbf{W}'_t) = \frac{\langle N_{\alpha\beta}\rangle}{\left(2\pi\left\langle w^2_{\alpha\beta}\right\rangle\right)^{3/2}} \times \exp\left[-\frac{\left(W'_n - \left\langle \widetilde{W}_n\right\rangle\right)^2}{2\left\langle w^2_{\alpha\beta}\right\rangle}\right]\exp\left[-\frac{\left|\mathbf{W}'_t - \left\langle \widetilde{\mathbf{W}}_t\right\rangle\right|^2}{2\left\langle w^2_{\alpha\beta}\right\rangle}\right], \tag{37}$$

where $\left\langle w^2_{\alpha\beta}\right\rangle$ is averaged square of turbulent relative velocity between two particles (24).

From expressions (36) and (37) we obtain closed form for PDF of reflected particles

$$\Phi_+(W''_n,\mathbf{W}''_t) = \frac{\chi\langle N_{\alpha\beta}\rangle}{\mu_n^2\mu_t\left(2\pi\left\langle w^2_{\alpha\beta}\right\rangle\right)^{3/2}} \times \exp\left[-\frac{\left(W''_n + \mu_n\langle \widetilde{W}_n\rangle\right)^2}{2\mu_n^2\left\langle w^2_{\alpha\beta}\right\rangle}\right]\exp\left[-\frac{\left|\mathbf{W}''_t - \mu_t\left\langle \widetilde{\mathbf{W}}_t\right\rangle\right|^2}{2\mu_t^2\left\langle w^2_{\alpha\beta}\right\rangle}\right], \tag{38}$$

Input flux of βth particles colliding with target particle is calculated on the base of PDF of particles before collision (37)

$$\begin{aligned}\left\langle \widetilde{W}_{n-}\right\rangle\langle N_{\alpha\beta}\rangle &= \int \mathrm{d}\mathbf{W}'_t\int_{-\infty}^{0} W'_n\Phi_-(W'_n,\mathbf{W}'_t)\,\mathrm{d}W'_n \\ &= \langle N_{\alpha\beta}\rangle\int_{-\infty}^{-\left\langle \widetilde{W}_n\right\rangle}\frac{w+\left\langle \widetilde{W}_n\right\rangle}{\left(2\pi\left\langle w^2_{\alpha\beta}\right\rangle\right)}\exp\left(-\frac{w^2}{2\left\langle w^2_{\alpha\beta}\right\rangle}\right)\mathrm{d}w \\ &= -\langle N_{\alpha\beta}\rangle\left\{\left\langle \widetilde{W}_n\right\rangle\left[1+\operatorname{erf}\left(\frac{\left\langle \widetilde{W}_n\right\rangle}{\sqrt{2\left\langle w^2_{\alpha\beta}\right\rangle}}\right)\right] + \sqrt{\frac{2}{\pi}\left\langle w^2_{\alpha\beta}\right\rangle}\exp\left(-\frac{\left\langle \widetilde{W}_n\right\rangle^2}{2\left\langle w^2_{\alpha\beta}\right\rangle}\right)\right\}.\end{aligned} \tag{39}$$

Output flux of βth particles reflected after collision from the target αth particle is calculated on the base of PDF (39)

$$\begin{aligned}\left\langle \widetilde{W}_{n+}\right\rangle\langle N_{\alpha\beta}\rangle &= \int \mathrm{d}\mathbf{W}''_t\int_0^{\infty} W''_n\Phi_+(W''_n,\mathbf{W}''_t)\mathrm{d}W''_n \\ &= -\chi\left\langle \widetilde{W}_{n-}\right\rangle\langle N_{\alpha\beta}\rangle.\end{aligned} \tag{40}$$

Boundary condition follows from equality of the sum of input (before collision) and output (after collision) fluxes to the flux with averaged relative velocity (33)

$$\left\langle \widetilde{W}_n\right\rangle\langle N_{\alpha\beta}\rangle = \left\langle \widetilde{W}_{n+}\right\rangle\langle N_{\alpha\beta}\rangle + \left\langle \widetilde{W}_{n-}\right\rangle\langle N_{\alpha\beta}\rangle. \tag{41}$$

From Eqs. (39)–(41) follows boundary condition

$$\left\langle \widetilde{W}_n \right\rangle \left[1 - \frac{1-\chi}{1+\chi} \operatorname{erf}\left(\frac{\left\langle \widetilde{W}_n \right\rangle}{\sqrt{2\left\langle w_{\alpha\beta}^2 \right\rangle}} \right) \right] = \frac{1-\chi}{1+\chi} \sqrt{\frac{2}{\pi}\left\langle w_{\alpha\beta}^2 \right\rangle} \exp\left(-\frac{\left\langle \widetilde{W}_n \right\rangle^2}{2\left\langle w_{\alpha\beta}^2 \right\rangle} \right). \quad (42)$$

Eq. (42) gives value of averaged relative velocity of dispersed phase as a function of average turbulent relative velocity between particles and probability of two particles association χ. It is necessary to note, that expressions (33) and (42) explicitly link gradient of particles concentration and averaged relative velocity of particles due to mass force.

For $\chi = 0$ (two particles after collision form new particle) the flux of βth particle on the target αth particle achieves maximal value. If $\chi = 1$ the particles after collision remain separate and flux on the target particle is zero $\langle \widetilde{W}_n \rangle = 0$.

If average relative velocity in radial direction is less than average fluctuation velocity in radial direction $\langle \widetilde{W}_n \rangle < \sqrt{2\langle w_{\alpha\beta}^2 \rangle/\pi}$ Eq. (42) turns out to simple boundary condition

$$\left\langle \widetilde{W}_n \right\rangle = \frac{1-\chi}{1+\chi} \sqrt{\frac{2}{\pi}\left\langle w_{\alpha\beta}^2 \right\rangle}. \quad (43)$$

Dimensionless velocity $\langle W_n^0 \rangle = \langle \widetilde{W}_n \rangle \Big/ \sqrt{2\langle w_{\alpha\beta}^2 \rangle/\pi}$ obtained as a solution of Eq. (42) and calculated on formula (43) is illustrated in Fig. 2. One can see that appreciable difference in dimensionless velocity $\langle W_n^0 \rangle$ received by two ways of calculations is observed for $\chi < 0.2$.

4.3. Coagulation kernel

Concentration of particles varies as a result of large number of particles collisions. Time scale of variation of averaged particles concentration is essentially grater than time scale between collisions of two particles. Taking this reasoning into consideration we calculate particles flux $\mathbf{J}_{\alpha\beta}$ in the quasi steady approximation. During our examination we assume that coefficient of relative diffusion of particles in Eq. (33) has constant value $D_{\alpha\beta}$, which is estimated at $\mathbf{y}_{\alpha\beta} = 0$. Also we neglect heterogeneity of βth particles concentration along angular coordinate θ (see Fig. 1). Result of our calculation can be treated only as estimation of real efficiency of coagulation of particles it turbulent flow. For quasi steady approximation in spherical coordinate system equation for $\langle N_{\alpha\beta} \rangle$ have the following form

$$-\frac{1}{4}\langle W_{\alpha\beta} \rangle \frac{\partial \langle N_{\alpha\beta} \rangle}{\partial r} = \frac{1}{r^2}\frac{\partial}{\partial r}\left(r^2 D_{\alpha\beta} \frac{\partial \langle N_{\alpha\beta} \rangle}{\partial r} \right), \quad (44)$$

where r is radial component of the relative vector $\mathbf{y}_{\alpha\beta}$ in coordinate system fixed at the centre of αth particle.

In Eq. (44) condition of particles collision is $\langle W_{\alpha\beta} \rangle > 0$. One multiplier 1/2 in the left-hand side of (44) appears as result of averaging the radial component of relative velocity $\langle \mathbf{W}_{\alpha\beta} \rangle$ along angular θ coordinate ($0 \leqslant \theta \leqslant \pi/2$, see Fig. 1). Another multiplier 1/2 in the left-hand side of (44) is ratio the area of upper half of the colliding sphere to the entirely area of the sphere.

First boundary conditions for Eq. (44) describe the asymptotic behavior of concentration

$$\langle N_{\alpha\beta} \rangle \to \langle N_{\alpha\beta}^0 \rangle \quad \text{for } r \to \infty. \quad (45)$$

Second boundary condition describes gradient of particles distribution on the surface of colliding sphere with radius $a_{\alpha\beta}$ (see Fig. 1). We used this boundary condition in linear form (43)

$$\frac{\langle W_{\alpha\beta} \rangle}{4}\langle N_{\alpha\beta} \rangle + D_{\alpha\beta}\frac{\mathrm{d}\langle N_{\alpha\beta} \rangle}{\mathrm{d}r} = \frac{1-\chi}{1+\chi}\sqrt{\frac{2}{\pi}\left\langle w_{\alpha\beta}^2 \right\rangle}\langle N_{\alpha\beta} \rangle \quad \text{for } r = a_{\alpha\beta}. \quad (46)$$

From solution Eq. (44) with boundary conditions (45) and (46) we find expression for flux (34) of βth particles on the surface of αth particle

$$J_{\alpha\beta} = \left(\frac{1-\chi}{1+\chi}\sqrt{\frac{2}{\pi}\left\langle w_{\alpha\beta}^2 \right\rangle} \right) \left[1 + \Theta_{\alpha\beta} \mathrm{e}^{\Theta_{\alpha\beta}} E_2(\Theta_{\alpha\beta}) \left(\frac{\frac{1-\chi}{1+\chi}\sqrt{\frac{2}{\pi}\left\langle w_{\alpha\beta}^2 \right\rangle}}{\langle W_{\alpha\beta} \rangle/2} - 1 \right) \right]^{-1},$$

$$\Theta_{\alpha\beta} = \frac{a_{\alpha\beta}\langle W_{\alpha\beta} \rangle/4}{D_{\alpha\beta}}. \quad (47)$$

The details of calculation of (47) are described in Appendix C. For $\chi = 1$ there no grows of αth particle as a result of collisions $J_{\alpha\beta} = 0$. If each collision between particles form new particle ($\chi = 0$) value of particles flux reaches a maximum value.

We shall consider the limiting cases for expression (47). Without mass forces driving particles $\langle W_{\alpha\beta} \rangle = 0$ we have $\Theta_{\alpha\beta} = 0$ and flux of βth particles is equal

$$J_{\alpha\beta} = \frac{1-\chi}{1+\chi}\sqrt{\frac{2}{\pi}\left\langle w_{\alpha\beta}^2 \right\rangle}.$$

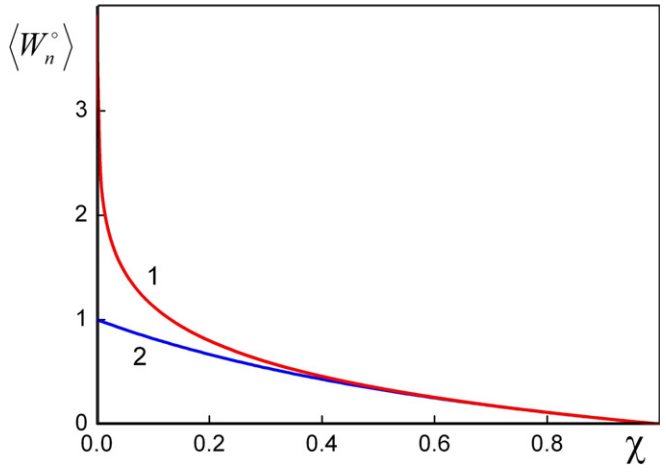

Fig. 2. Dimensionless averaged relative velocity as a function of probability of new particle formation: (1) solution of Eq. (42); (2) calculation on formula (43).

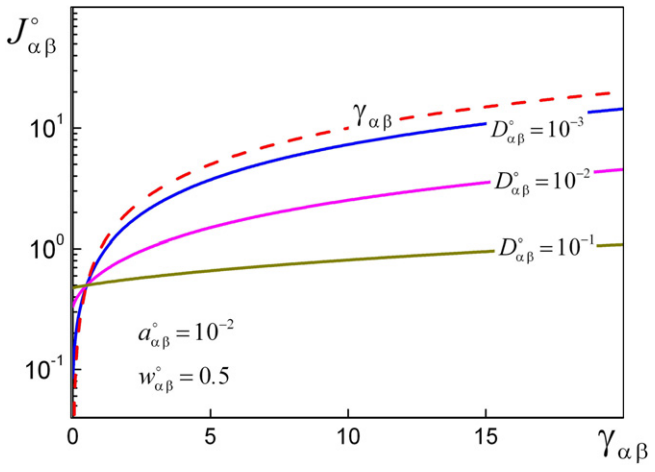

Fig. 3. Dimensionless particles flux as a function of dimensionless average relative velocity between particles.

Last result is similar to the expression for colliding velocity used in [2,12]. If average relative velocity is essentially grater than turbulent component $\langle W_{\alpha\beta}\rangle \gg \sqrt{\langle w^2_{\alpha\beta}\rangle}$, than $\Theta_{\alpha\beta}e^{\Theta_{\alpha\beta}}E_2(\Theta_{\alpha\beta}) \to 1$ [18], and we obtain

$$J_{\alpha\beta} \to \langle W_{\alpha\beta}\rangle/4.$$

It is worth to note, that turbulent component of relative velocity $\sqrt{2\langle w^2_{\alpha\beta}\rangle/\pi}$ is equal to the average radial velocity for Gaussian distribution (see Appendix B).

Coagulation kernel is sum of particles flux over surface of colliding sphere with radius $a_{\alpha\beta}$

$$K_{\alpha\beta} = 4\pi(a_\alpha + a_b)^2 J_{\alpha\beta}.$$

Fig. 6 illustrates the influence of coefficient of relative turbulent diffusion between particles on the flux $J_{\alpha\beta}$. On the Fig. 3 dimensionless variables are $J^0_{\alpha\beta} = J_{\alpha\beta}/u$, $\gamma_{\alpha\beta} = \langle W_{\alpha\beta}\rangle/(4u)$, $w^0_{\alpha\beta} = (1-\chi)/(1+\chi)\sqrt{2\langle w^2_{\alpha\beta}\rangle/(\pi u^2)}$, $a^0_{\alpha\beta} = a_{\alpha\beta}/L_E$, $D^0_{\alpha\beta} = D_{\alpha\beta}/(uL_E)$($L_E$ is integral space macro scale). One can see that for small level of turbulence particles flux is governed by average relative velocity between particles $\gamma_{\alpha\beta}$. Fig. 3 we also illustrate, that for small value of average relative velocity $\gamma_{\alpha\beta} < 1$ the flux is control by turbulent relative velocity $w^0_{\alpha\beta}$.

In the gravity field average relative velocity is noticeable for particles with distinct radiuses. Chaotic motion of such particles is little correlated, and value of coefficient of relative turbulent diffusion of particles is nonzero, that leads to decreasing the particles flux in comparison with coagulation without turbulence (Fig. 3). This effect may be explained as follows. Probability of collision of βth particle with target αth particle is reduced at increasing heir relative chaotic motion.

5. Calculation results

We compare our theoretical results with DNS data [2,3,19]. DNS calculation was realized for various Reynolds turbulent numbers. For $Re_\lambda \approx 25$ universal region in turbulent spectra is diminishing in comparison with larger Reynolds numbers (see Appendix A). Considering this fact we expect satisfactory agreement our results with DNS data obtained for larger Reynolds number. On the Fig. 4 is shown dependence of response function (10) on parameter of particles inertia. From Fig. 4 one can conclude that increasing dimensionless parameter of particles velocity slip $\gamma_\alpha = \langle W_\alpha\rangle/u$ decrease intensity of turbulent particles motion.

Correlation coefficient between turbulent velocities of two identical particles is decreasing with increasing particles inertia (Fig. 5). In Fig. 5 also shown the DNS data for small Reynolds number of turbulence $Re_\lambda \approx 25$. One can see that values of these DNS data essentially differ from data obtained for larger Re_λ . Our theoretical data coordinated reasonably with DNS data for $Re_\lambda \geqslant 45$.

Averaged module of relative velocity between particles is composition of two effects. First, increasing the particles inertia monotonically reduced correlation between its chaotic motion, and intensity of turbulent relative velocity increases (Fig. 6). For particles with dynamic relaxation times of order integral time scale of turbulence $\tau_\alpha \propto T_E$ the averaged module of relative velocity reaches a maximum value. Second, the further grows of particle inertia suppresses chaotic motion of particles, and turbulent relative velocity between particles reduced. It is necessary to note, that for inertia less particles DNS data [2] includes turbulent velocity difference at the Kolmogorov micro scale $\approx\eta_K$, so for $\Omega_\alpha = 0$ DNS data distinct from zero.

For particles with different values of inertia parameters the behavior of turbulent relative velocity between particles is more complex (see Fig. 7). Fig. 7 present dependence of average module of turbulent relative velocity on inertial parameter of αth particles provided that inertial parameter of βth particle is fixed. One can see nonmonotonic dependence of relative velocity on αth particles inertia. Turbulent

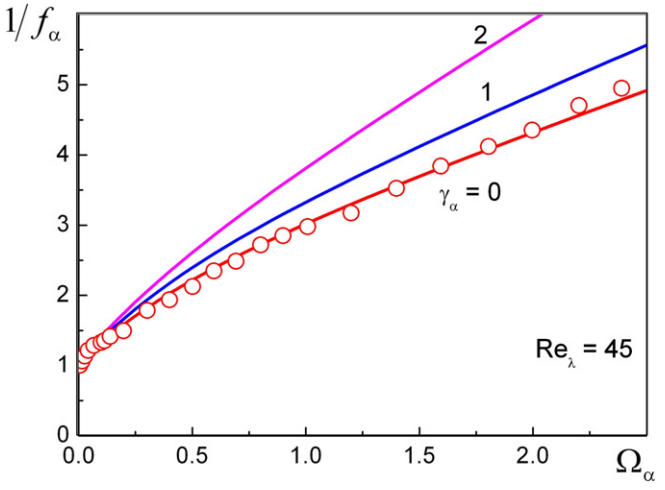

Fig. 4. Particle response function (10) with various parameters of velocity slips as a function of particles inertia. Lines are model predictions, points are DNS data [19] for $\gamma_\alpha = 0$.

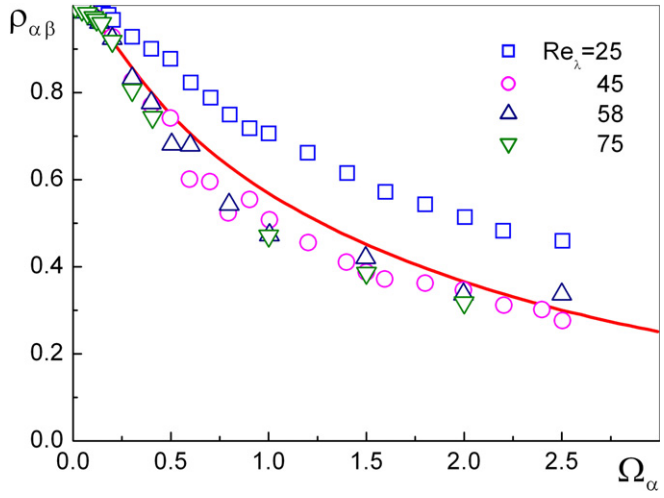

Fig. 5. Correlation coefficient of identical particles as a function of their inertia parameters. Line is model predictions, points are DNS data [2].

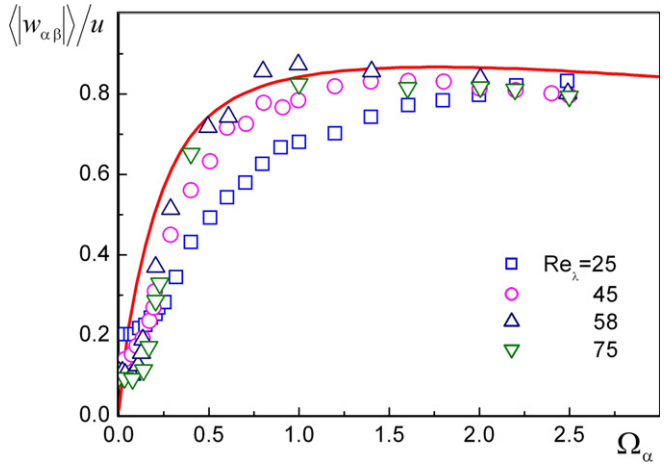

Fig. 6. Dependence of average module of turbulent relative velocity for identical particles on particles inertia. Line is model predictions, points are DNS data [2].

motion of particles with close inertial parameters $\tau_\alpha \approx \tau_\beta$ correlates more than particles with different inertial parameters. This fact connected with minimum value of the relative velocity in Fig. 7(a) and (b). For βth particle with $\tau_\beta \propto T_E$ relative velocity reaches a maximum value if inertia parameters of αth particles are essentially below the inertial parameter of βth particle (Fig. 7(a)). Further growth of αth particles inertia parameters $\Omega_\alpha \gg 1$ leads to constant intensity of chaotic relative motion between particles (Fig. 7(a) and (b)). For region $\Omega_\alpha \gg \Omega_\beta$ module of turbulent relative velocity is determined by intensity of turbulent motion of particles with smaller parameter of inertia. When parameter of inertia βth particles is smaller than integral time scale $\Omega_\beta \ll 1$ the minimum value of relative velocity module is shift to the region with minor values $\Omega_\alpha \ll 1$ (Fig. 7(b)). The minimum value of relative velocity is sufficiently less than in the case when $\Omega_\beta \propto 1$. For great parameters of inertia αth particles $\Omega_\alpha \gg 1$ the intensity of relative motion aspires to constant value. These tendencies prove to be true for particles with small inertia in Fig. 8.

Reasonable agreement our theoretical results with DNS data [2,3,19] testify to validity of the developed model for calculation the coagulation process of polydisperse droplets in various turbulent flows. We analyzed two different cases of turbulent flows: turbulence in a cloud and turbulence in a pipe in the assumption of isotropy. In the last case we also investigated two situations: turbulent motion of droplets in gravitational field and turbulent motion of droplets without gravitation.

First, we present the results for turbulence in clouds with following parameters (see, for example [20]): turbulent dissipation rate is $\varepsilon = 500\ \mathrm{cm^2/s^3}$ and Reynolds number of turbulence is $Re_\lambda = 4000$. Other parameters of turbulence are calculated with the help of Appendix A. Mean velocity of turbulence is $u = 0.95$ m/s, Kolmogorov time micro scale $\tau_K = 17.3$ ms, integral time scale of turbulence is $T_E = 8.7$ s.

Coefficient of aerodynamic resistance of spherical droplets is calculated with nonlinear effects. Fig. 9 illustrated the

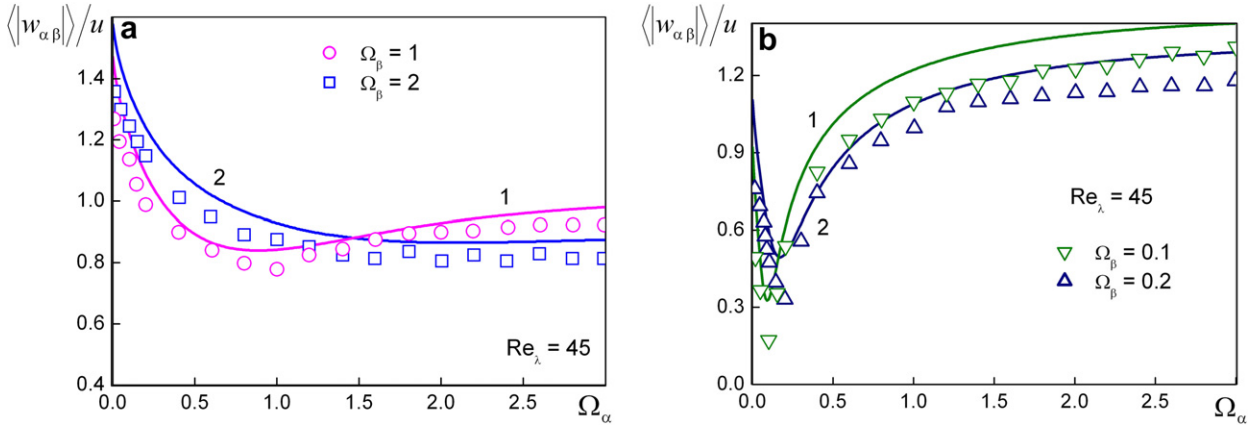

Fig. 7. Module of turbulent relative velocity between two particles as a function of inertia αth particle (a). (b) Inertial parameter of βth particle is shown on the figure. Points are DNS data [3]. Lines are model predictions: (a) 1 – $\Omega_\beta = 1$, 2 – 2; (b) 1 – $\Omega_\beta = 0.1$, 2 – 0.2.

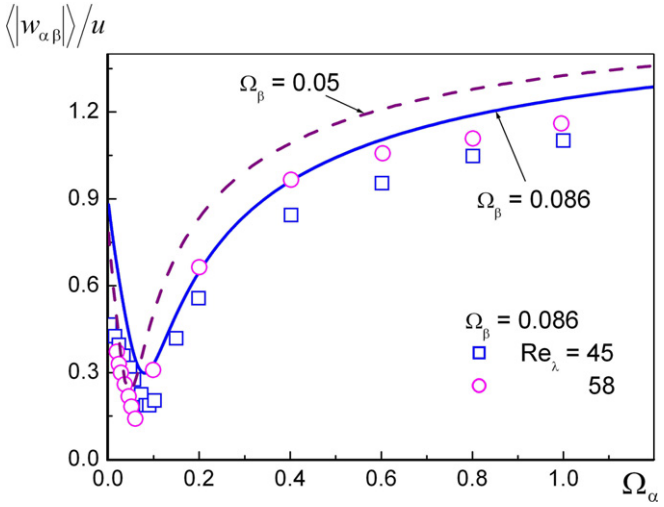

Fig. 8. Module of turbulent relative velocity between two particles as a function of inertia αth particle. Inertial parameter of βth particle is shown on the figure. Lines are model predictions, points are DNS data [3].

main dynamical characteristics of droplets in the case of cloud turbulence. Result of calculations with Stokes approach and linear resistance are essentially different not only for average relative velocity (Fig. 9(a)), particles relaxation times (Fig. 9(b)), but also for parameter of droplet inertia (Fig. 9(c)) and response function (Fig. 9(d)). In most investigated diapason of droplets diameters sedimentation velocity is surpass the mean turbulent velocity (Fig. 9(a)), so one can expect noticeable influence of crossing trajectory effect on turbulent characteristics of droplets. Droplets relaxation time is less than integral time scale of turbulence (Fig. 9(b)), so parameter of droplets inertia is smaller than unity (Fig. 9(c)). Droplets response function is essentially higher than zero (Fig. 9(d)), and intensity of droplets turbulence is high enough. So, rather large values of sedimentation velocities of droplets will reduce their coefficients of turbulent diffusion.

In Fig. 10 are present relative turbulent parameters of droplets at a cloud conditions. Average module of relative turbulent velocity and coefficient of relative diffusion of droplets rapidly varies in the diapason when diameters of droplets are close to each other (Fig. 10(a) and (b)). For larger difference between droplets diameters relative turbulent velocity and coefficient of relative diffusion vary insignificantly. One can notice that for droplets with equal diameters coefficient of turbulent diffusion is suppressed as a result of crossing trajectory effect. Values of turbulent

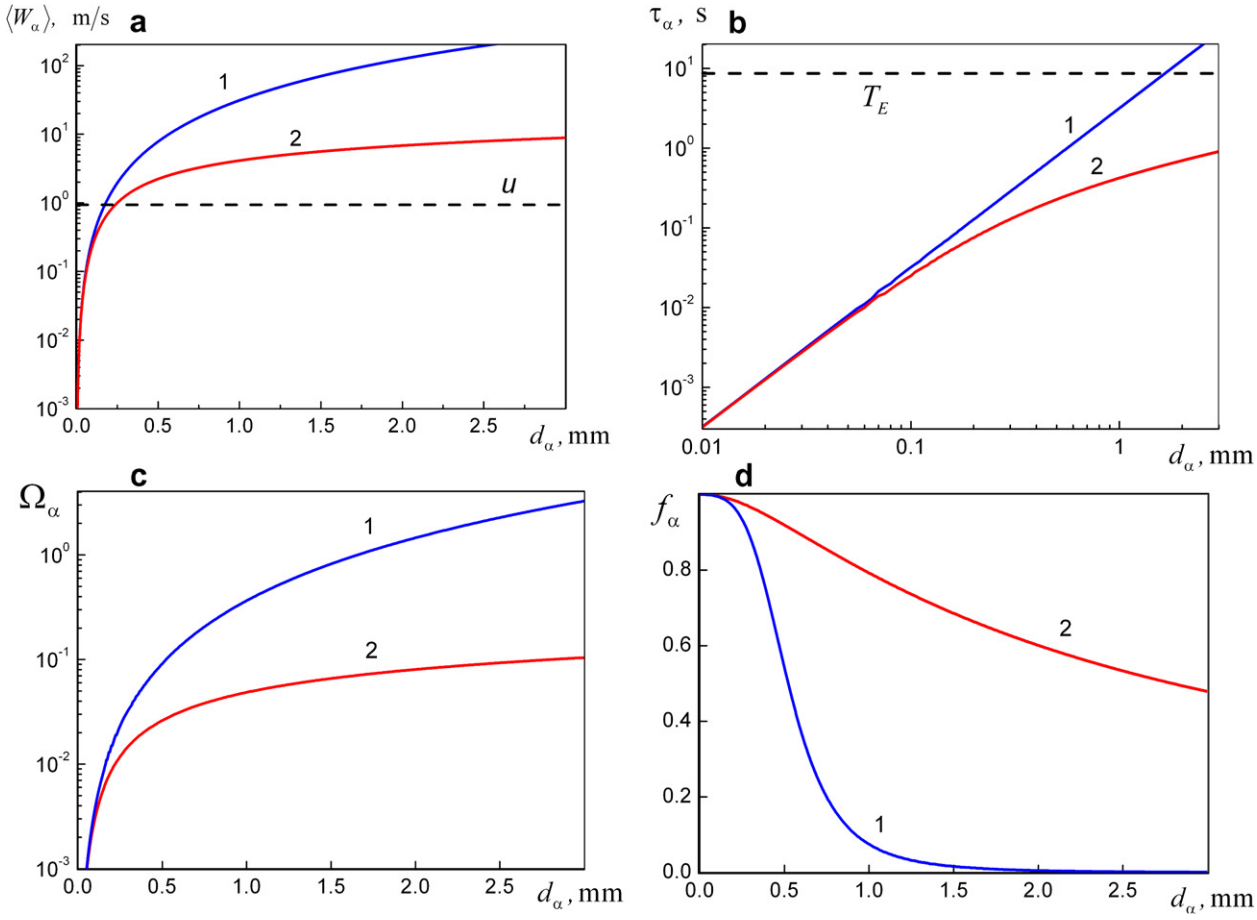

Fig. 9. Characteristics of droplets in cloud turbulence. Average relative velocity due to gravity (a). Droplets relaxation times (b). Parameter of droplets inertia (c). Droplets response function (d). Lines are calculation results: (1) Stokes drag; (2) nonlinear drag.

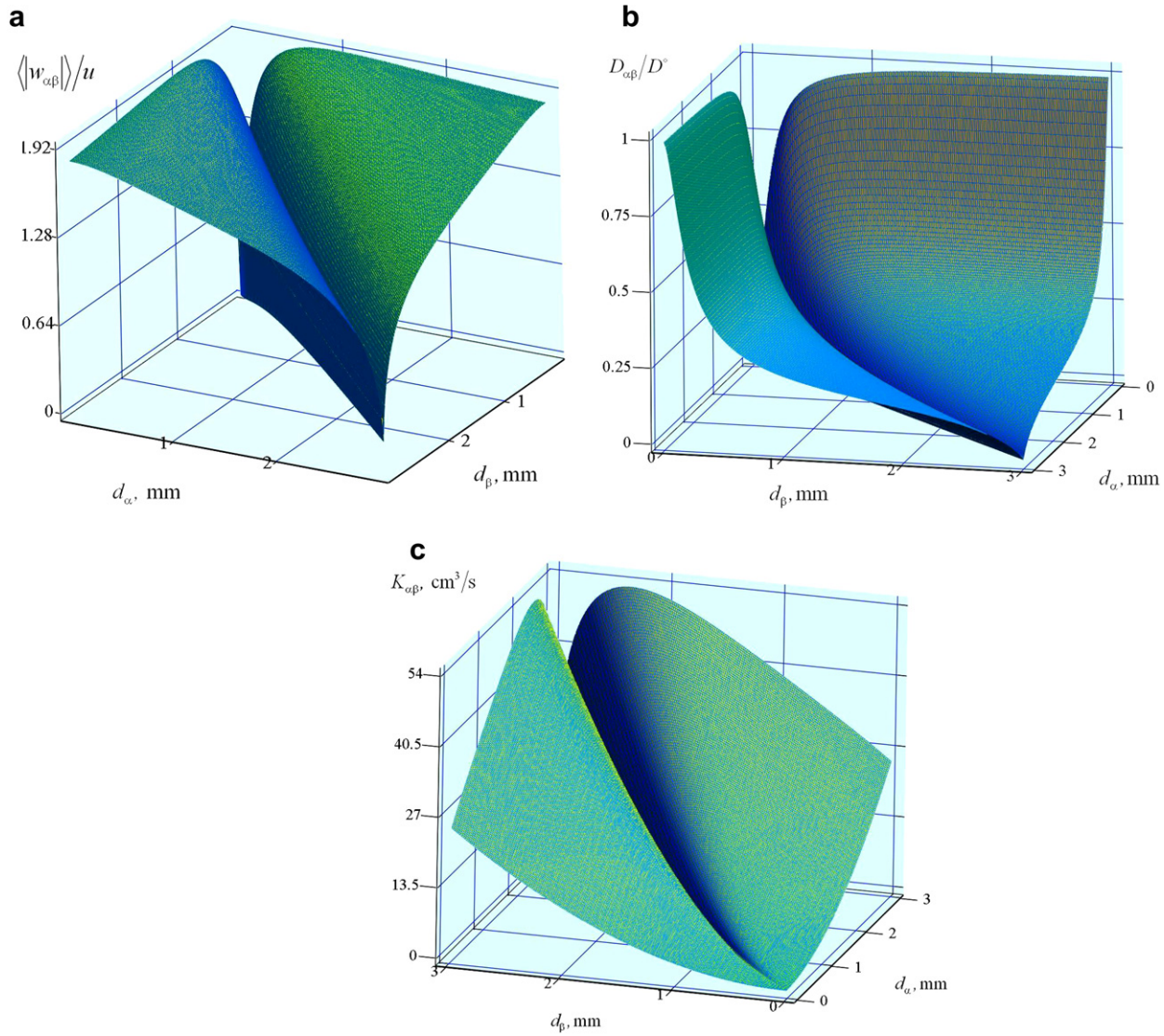

Fig. 10. Parameters of relative turbulent motion of droplets in cloud turbulence. Averaged module of turbulent relative velocity (a). Coefficient of relative turbulent diffusion (b). Kernel of coagulation (c).

relative velocity and turbulent diffusion for droplets with sufficiently distinct diameters are comparable with values of corresponding characteristics of carrier phase turbulence. Contribution of turbulent effects and gravitational sedimentation of droplets in coagulation kernel are shown in Fig. 10(c). Rapid change of coagulation coefficient in the diapason when diameters of droplets are close to each other is connected with analogous behavior of relative turbulent velocity.

For comparison in Fig. 11 is shown coagulation kernel due to droplets sedimentation velocity without turbulence. It is principal differences between two pictures. On the one hand, droplets with equal diameters will coagulate only in turbulent flow. However on the other hand, from Figs. 10(c) and 11 one can notice, that for droplets with appreciable difference in their diameters turbulence reduces coagulation kernel in comparison with pure gravitational coagulation.

For cloud turbulence Fig. 12 illustrates behavior of averaged module of relative velocity between droplets when diameter of βth droplet is set. For droplets 0.01 mm $\leqslant d_\alpha \leqslant$ 3 mm average module of relative velocity between droplets of equivalent diameters growth with increasing droplets sizes (curve 1). In the narrow diapason of droplets sizes the module of turbulent relative velocity grows rapidly with increasing the difference between droplets diameters. For larger difference in droplets sizes the value of module of relative velocity is determined by intensity of turbulent motion of smaller droplet (Fig. 12).

Contribution of relative turbulent motion of droplets has important contribution in coagulation kernel (Fig. 13). Coagulation of droplets with identical diameters is possible only due to turbulence (curve 1). Coagulation rate of droplets with various small diameters also determines by chaotic relative motion. There is a range of droplets diameters, when turbulence sufficiently increases

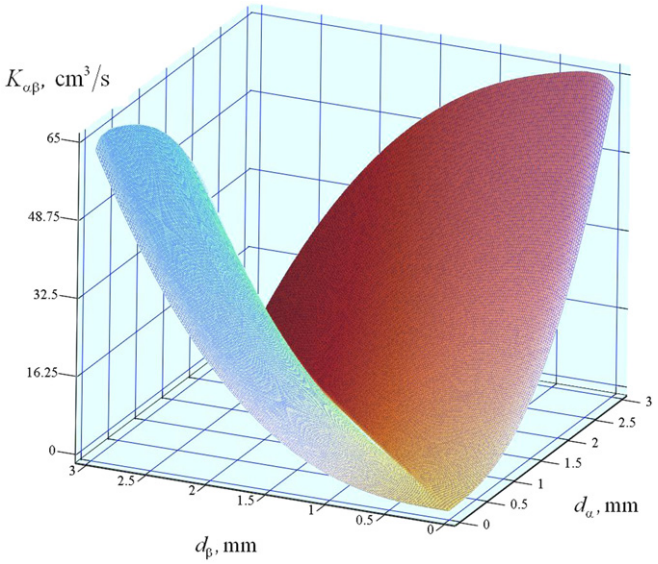

Fig. 11. Gravitational coagulation kernel without turbulence.

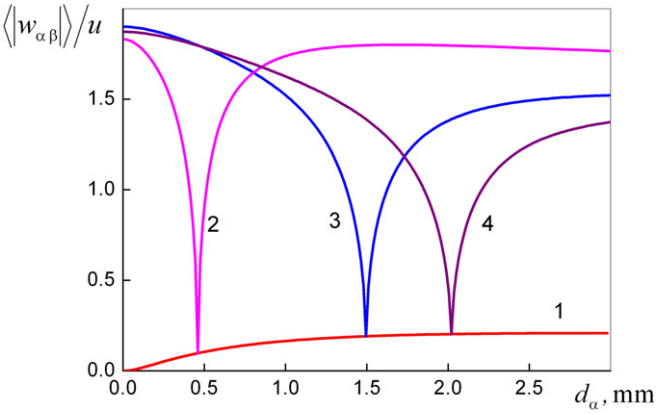

Fig. 12. Average module of relative turbulent velocity as a function of diameter of αth droplets when diameter of βth droplet is fixed. Lines are model predictions: (1) droplets with identical diameters; (2) $d_\beta = 0.46$ mm; (3) 1.5 mm; (4) 2 mm.

coagulation rate (see lines 4 in Fig. 13). But there is other diapason of droplets diameters when total coagulation kernel is smaller then in the case of pure gravitational coagulation (see lines 2 and 3 in Fig. 13).

Second case, which we consider, illustrates droplets behavior for conditions similar to the turbulence in pipes flow. We carried out our investigation in the assumptions of stabilized conditions and isotropic turbulence. We set turbulent dissipation rate $\varepsilon = 5 \times 10^4$ cm^2/s^3, Reynolds number of turbulence $Re_\lambda = 100$. Estimation of other turbulence parameters give: mean velocity of turbulence is $u = 0.47$ m/s, Kolmogorov time micro scale $\tau_K = 1.7$ ms, integral time scale of turbulence is $T_E = 22$ ms. In that case diapason of diameters of droplets involving in turbulent motion is sufficiently narrow than in previous study. Two factors suppressed turbulent motion of droplets. First, in

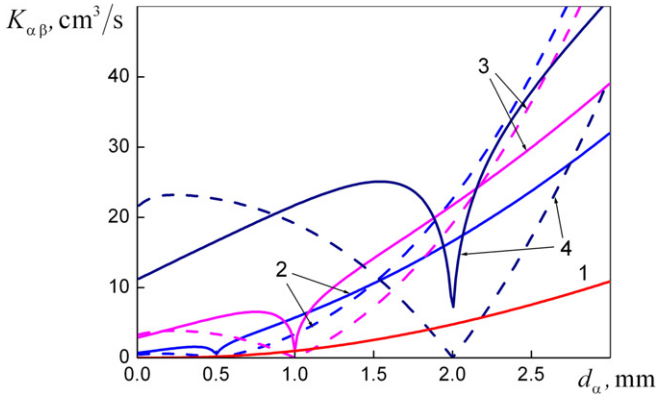

Fig. 13. Coagulation kernel as a function of droplets diameters of αth particles when diameter of β droplet is fixed. Lines model predictions. Solid lines for turbulent coagulations, dashed lines for only gravitational coagulations: (1) droplets with equivalent diameters: (2) $d_\beta = 0.5$ mm; (3) 1 mm: (4) 2 mm.

most part of the range of diameters sedimentation velocity of droplets is larger that mean turbulent velocity (Fig. 14(a)). And second, in the most part of droplets diameters value of relaxation time is larger then integral time scale of turbulence (Fig. 14(b)). Hence crossing trajectory effect and high values of parameter of droplets inertia (Fig. 14(c)) sufficiently reduced response function of large droplets (Fig. 14(d)).

Fig. 15 illustrates relative turbulent parameters for pipe flow conditions. On the picture of average module of relative velocity (Fig. 15(a)) there is a maximum in the region of closed values of droplets diameters. Growth of difference between droplets sizes leads, first, to reduction of correlation coefficient between droplets chaotic motion (Fig. 15(b)) and, second, to increasing turbulent relative velocity between droplets (Fig. 15(a)). It is necessary to pay attention that in gravitational field correlation coefficient is not reduced with increasing diameters of droplets with equal size. This feature in behavior of correlation coefficient is traced only in mass force fields (compare Fig. 15(a) and Fig. 5). Coefficient of relative turbulent diffusion of droplets also has a maximum value (Fig. 15(c)). As against a case of cloud turbulence average relative velocity and coefficient of turbulent relative diffusion change with droplets diameters variation more smooth. Also in distinct of cloud turbulence the coagulation kernel depends on droplets diameters without sharp corners (compare Fig. 10(c) and 15 (d)).

On the Fig. 16 are shown results of parametric study of average module of turbulent relative velocity between droplets. One can notice, that a maximum value in the relative velocity of identical droplets (curve 1) is localized at the diameter which is corresponds to the value of parameter of droplets inertia $\Omega_\alpha \approx 1$ (compare Figs. 12 and 16). Increasing difference between droplets diameters leads to a constant value of turbulent relative velocity. Existence of the maximum value in dependence of coefficient of relative turbulent diffusion for identical droplets is confirmed

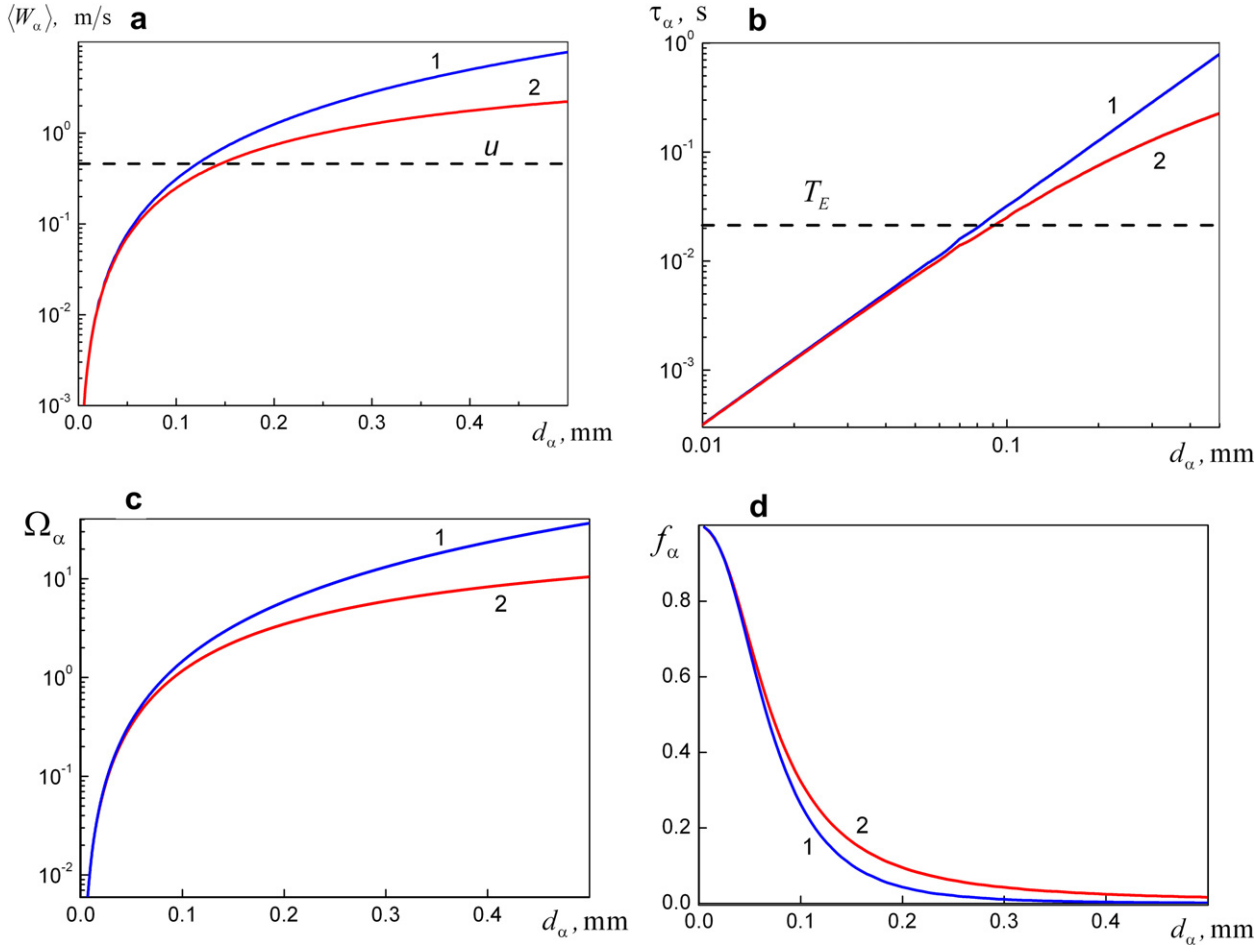

Fig. 14. Characteristics of droplets in a pipe flow turbulence. Sedimentation velocities of droplets (a). Droplets relaxation times (b). Parameters of droplets inertia (c). Response functions of droplets (d). Lines are calculation results: (1) Stokes drag; (2) nonlinear drag.

by the Fig. 17. Initial grows of relative diffusion is connected with destruction of correlation between turbulent motion of droplets with increasing in their sizes (see Fig. 15 (b) and (17)). The subsequent decreasing of diffusion coefficient is explained by crossing trajectory effect.

At the analysis of coagulation kernel (Fig. 18) we can distinct two regions in droplets diameters. In the first region total turbulent coagulation kernel is larger then gravitational kernel without turbulence. In that region value of turbulent relative velocity between droplets surpass difference in their sedimentation velocities. In second region is observed reduction of total turbulent coagulation kernel in comparison of pure gravitational coagulation. This effect is connected with relative turbulent diffusion between droplets.

Fig. 19 illustrates the characteristic features of droplets relative motion in the turbulent flow without gravitational forces. Parameters of turbulence are analogous to the case of pipe flow. Without gravitation parameter of particles inertia coincides with the parameter calculated in Stokes approximation (see Fig. 14(c)). In opposition to the previous case correlation coefficient aspires to zero value for large droplets (compare Fig. 15(b) and 19(a)). Zero value of gravitation forces and therefore absence of crossing trajectories effect lead to the constant value of coefficient of relative turbulent diffusion for larger droplets (Fig. 19(b)). Coagulation coefficient smoothly varies with increasing droplets diameter (Fig. 19(c)).

Fig. 20 presents calculation results for gravitational coagulation kernel without turbulence. Comparison of Fig. 13 with 18 and Figs. 10(c), 15(d), 19(c) with Figs. 11, 20 allows to draw following conclusions about the responsibility of the two distinct mechanisms in droplets coagulation.

1. Coagulation of droplets with equal diameters is possible only due to its turbulent motion. Involving of droplets into turbulent motion of energy containing eddies is origin of chaotic relative velocity between droplets. Turbulent coagulation of droplets may proceed at the absence of mass forces.
2. Turbulent relative diffusion between droplets may reduce the value of coagulation kernel for droplets with sufficient difference in their sizes. Simple hypothesis

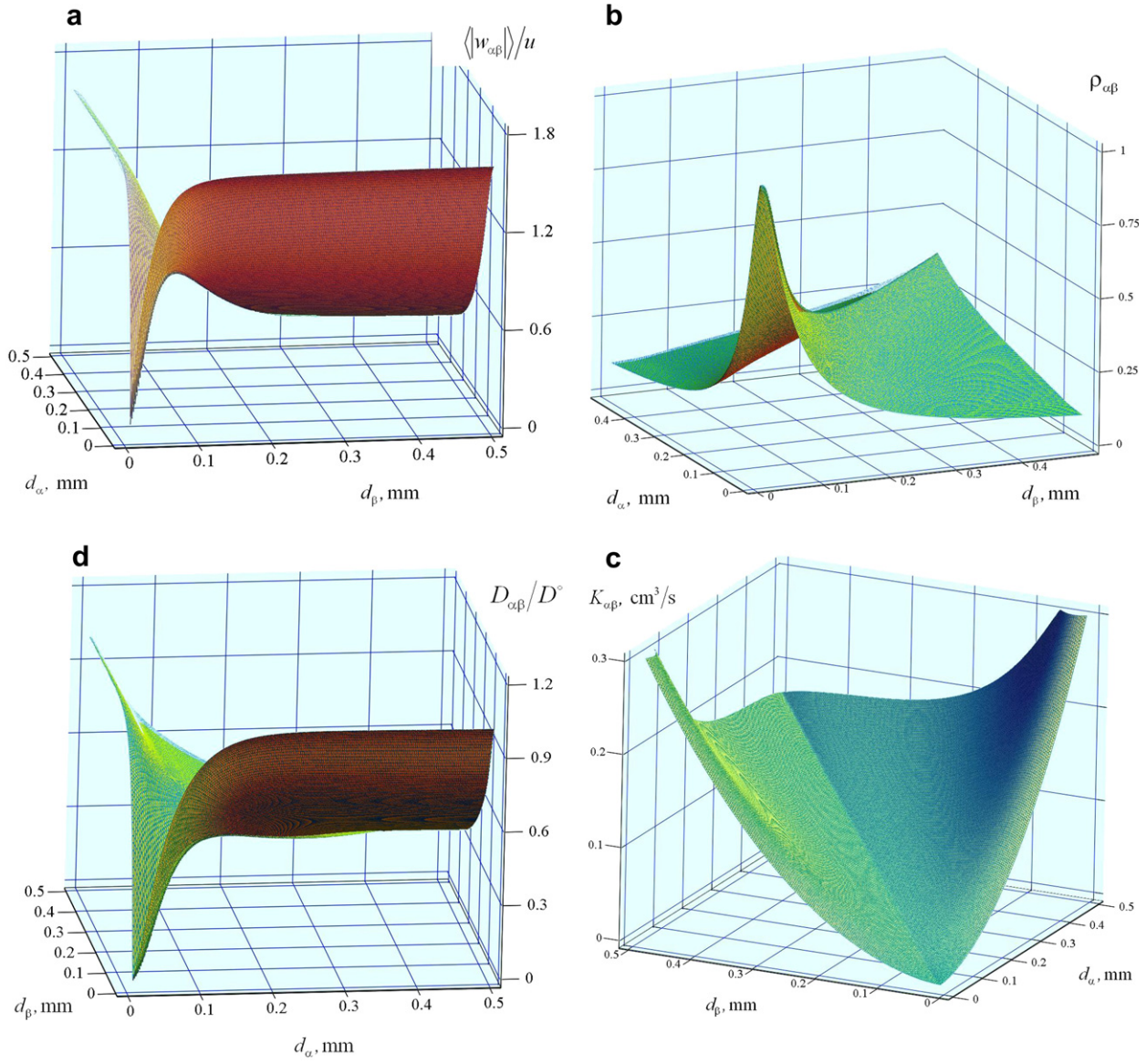

Fig. 15. Parameters of relative turbulent motion of droplets. Average module of turbulent relative velocity (a). Correlation coefficient (b). Coefficient of turbulent relative diffusion (c). Coagulation kernel (d).

about additivity of two mechanisms of droplets coagulation is incorrect.

3. Qualitative and quantitative features of turbulent relative motion of droplets and values of coagulation kernel is strongly depends on types of turbulent flows. For example, essentially different results are obtained for parameters characteristics to cloud turbulence and turbulence in a pipe flow.

6. Conclusions

Euler description is used for investigation particles chaotic motion in turbulence. Spectral presentation of a carrier phase velocity fluctuations is used for calculation turbulent characteristics of particles. On the base of PDF approach the boundary condition takes into account momentum loss and probability of particles association is obtained. Expression for turbulent coagulation kernel of particles in gravity field is found out. It is proved that relative turbulent diffusion of particles may decrease coagulation coefficient in comparison of pure gravitational coagulation.

Two distinct conditions of turbulence are considered. Turbulence in a cloud and turbulence in pipe flow at stabilized condition in isotropic assumption are studied. It is found that qualitative and quantitative features of relative motion of particles strongly depend on type of turbulence.

Results of present work are valid for particles with dynamic relaxation times larger than Kolmogorov time micro scale. Effects connected with preferential concentration of particles are realized for particles with smaller relaxation times and will be considered in next publication.

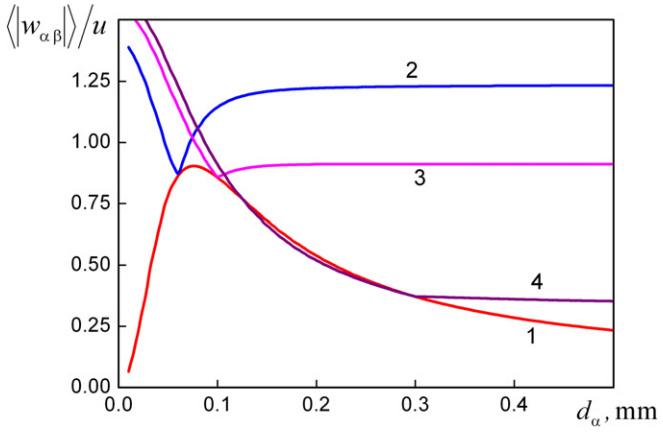

Fig. 16. Average module of relative turbulent velocity as a function of diameter of αth droplets when diameter of βth droplet is fixed. Lines are model predictions: (1) droplets with identical diameters; (2) $d_\beta = 0.06$ mm; (3) 0.1 mm; (4) 0.3 mm.

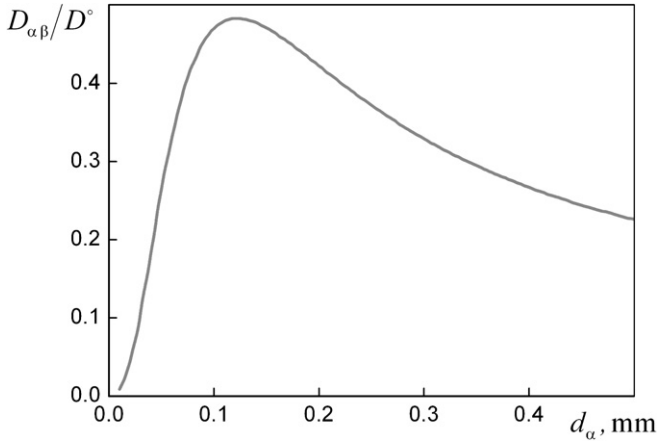

Fig. 17. Coefficient of relative turbulent diffusion between droplets with equal diameters.

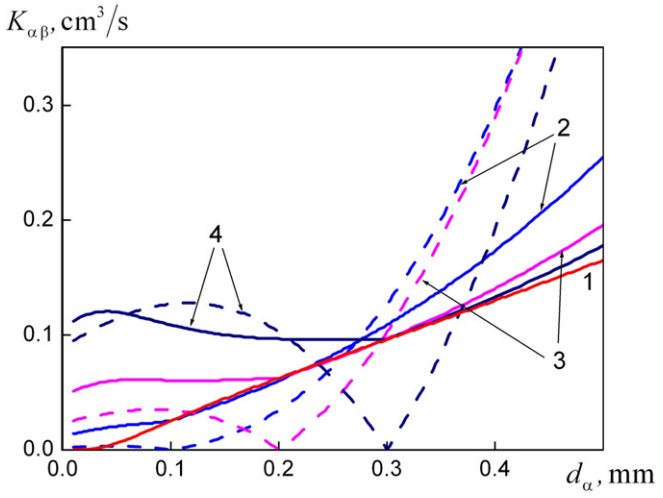

Fig. 18. Coagulation kernel as a function of droplets diameters of αth particles when diameter of β droplet is fixed. Lines model predictions. Solid lines for turbulent coagulations, dashed lines for only gravitational coagulations without turbulence: (1) droplets with equivalent diameters: (2) $d_\beta = 0.1$ mm; (3) 0.2 mm: (4) 0.3 mm.

Appendix A. Turbulence spectrum for energy containing eddies

For statistically stationary and homogeneous turbulence the spectral form of two-point and two-time correlation function of gas velocity fluctuations in Euler description is defined as follows

$$\langle u_i(\mathbf{x}+\mathbf{y}, t+s)u_j(\mathbf{x},t)\rangle = E_{ij}(\mathbf{y},s) = \int \mathrm{e}^{\mathrm{i}\mathbf{k}\cdot\mathbf{y}}\hat{E}_{ij}(\mathbf{k},s), \quad (A.1)$$

$$\hat{E}_{ij}(\mathbf{k},s) = \frac{1}{(2\pi)^3}\int \mathrm{e}^{-\mathrm{i}\mathbf{k}\cdot\mathbf{y}}E_{ij}(\mathbf{y},s),$$

where $\widehat{E}_{ij}(\mathbf{k},s)$ is spectral presentation of velocity correlation function; $\mathbf{k}$ is a wave vector.

For isotropic turbulent flow function $\widehat{E}_{ij}(\mathbf{k},s)$ in (A.1) have a general form [14]

$$\widehat{E}_{ij}(\mathbf{k},s) = \widehat{E}_{ij}(k,s) = \frac{\widehat{E}(k,s)}{4\pi k^2}\left(\delta_{ij} - \frac{k_i k_j}{k^2}\right), \quad (A.2)$$

where δ_{ij} is Kronecker delta; $k^2 = k_i k_i$ is square of module of a wave vector.

Function $\widehat{E}(k,s)$ in (A.2) describes distribution of turbulent energy along the eddies with characteristic space scale $\approx k^{-1}$. In spectral presentation one point velocity correlation and turbulent energy of carrier phase are

$$\langle u_i(\mathbf{x},t+s)u_j(\mathbf{x},t)\rangle = \int \widehat{E}_{ij}(\mathbf{k},s)\,\mathrm{d}\mathbf{k} = \int_0^\infty \widehat{E}_{ij}(k,s)\,\mathrm{d}k,$$

$$E = \int_0^\infty \widehat{E}(k,0)\,\mathrm{d}k. \quad (A.3)$$

We consider particles dynamic relaxation times of which are comparable with integral time scale of turbulent energetic eddies. For modeling spectra of energy containing region we used von Carman approximation (see, for example [14])

$$\widehat{E}_{\mathrm{E}}(k,s) = \widehat{E}^0_{\mathrm{E}}(k)\exp(-\omega_k s),$$

$$\widehat{E}^0_{\mathrm{E}}(k) = E\frac{g_{\mathrm{E}}}{k_{\mathrm{E}}}\frac{x^4}{(1+x^2)^{17/6}}, \quad (A.4)$$

where $\widehat{E}^0_{\mathrm{E}}(k)$ is Carman's approximation of three-dimensional spectra of turbulence; k_{E} is wave vector of energy containing eddies; ω_k is frequency of eddies; $x = k/k_{\mathrm{E}}$ is dimensionless wave number; E is turbulent energy.

In the region of energy containing eddies ($0 < x \leqslant 1$) $\widehat{E}^0_{\mathrm{E}} \propto k^4$. The universal region of turbulent spectra ($x \gg 1$) is describes with the well-known Kolmogorov distribution

$$\widehat{E}^0_{\mathrm{E}}(k) = C_{\mathrm{K}}\varepsilon^{2/3}k^{-5/3}, \quad (A.5)$$

where C_{K} is Kolmogorov constant; ε is turbulent dissipation rate.

From (A.4) and (A.5) at $x \gg 1$ follows the expression for scale of wave vectors for energy containing eddies

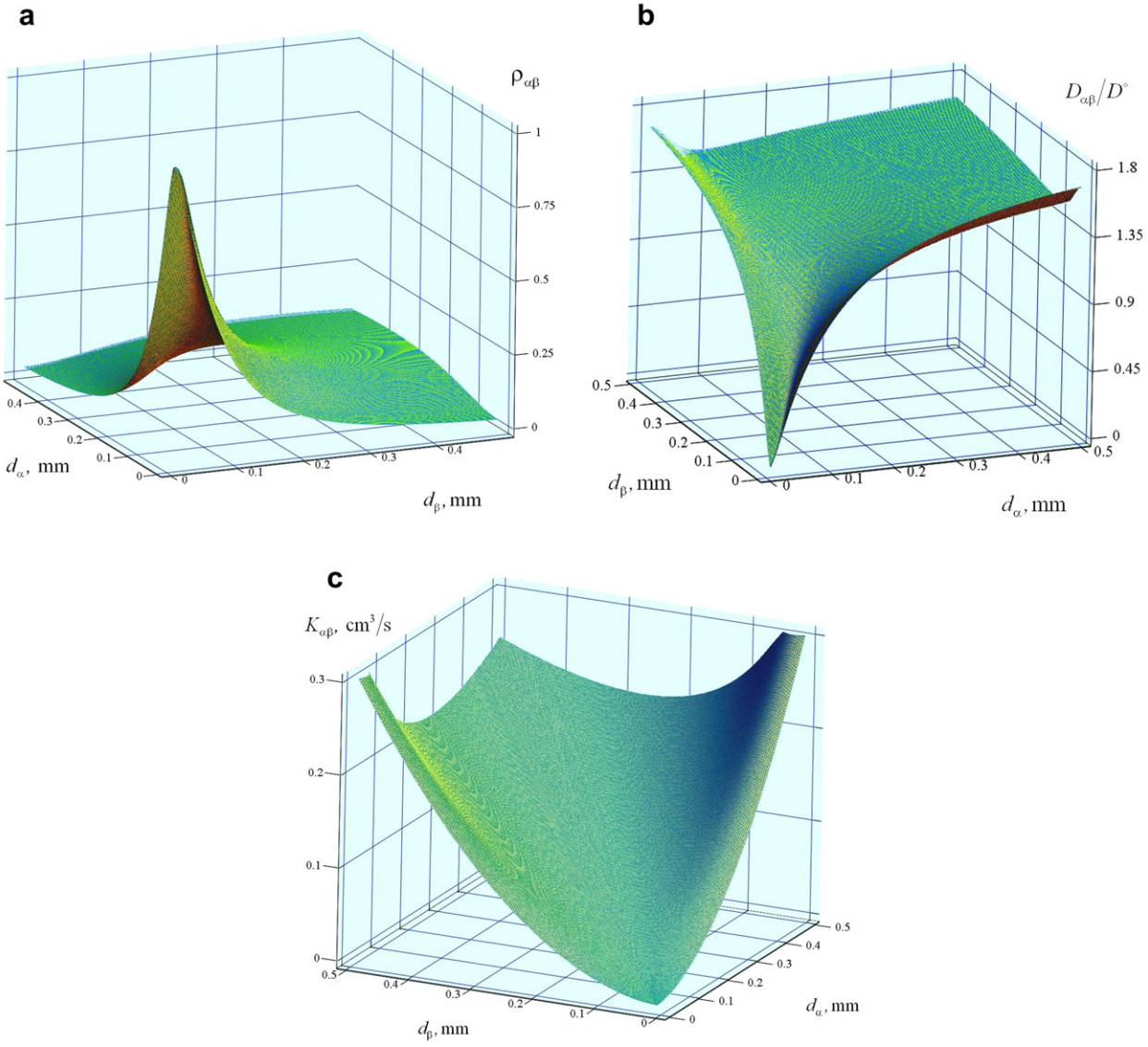

Fig. 19. Parameters of relative turbulent motion of droplets without gravitation. Coefficient of correlation (a). Coefficient of relative turbulent diffusion of droplets (b). Coagulation kernel (c).

$$k_{\mathrm{E}} = \left(\frac{C_{\mathrm{K}}}{g_{\mathrm{E}}}\right)^{2/3} \frac{\varepsilon}{E^{3/2}}. \tag{A.6}$$

The normalization constant g_{E} in (A.4) is calculated from the conditions (A.3)

$$E = \int_0^\infty \widehat{E}_E^0(k)\,\mathrm{d}k, \quad g_{\mathrm{E}} = \frac{2}{B(5/2,1/3)} \approx 0.969.$$

Here $B(x,y)$ is beta function

$$B(x,y) = \int_0^\infty \frac{\theta^{x-1}}{(1+\theta)^{x+y}}\,\mathrm{d}\theta.$$

The frequency of energy containing eddies is estimated under hypothesis about cascade transfer of turbulent energy along the spectra

$$\omega_k = \varepsilon^{1/3} k_{\mathrm{E}}^{2/3} x^{2/3}. \tag{A.7}$$

Integral time scale of turbulence is calculate along the approximation (A.4)

$$T_{\mathrm{E}} = \frac{1}{E}\int_0^\infty \mathrm{d}k \int_0^\infty \widehat{E}_{\mathrm{E}}(k,s)\,\mathrm{d}s = \frac{1}{E}\int_0^\infty \frac{\widehat{E}_{\mathrm{E}}^0(k)}{\omega_k}\,\mathrm{d}k = \beta_{\mathrm{E}}\frac{E}{\varepsilon}. \tag{A.8}$$

After calculation the last integral we obtain

$$\beta_{\mathrm{E}} = \frac{g_{\mathrm{E}}}{2} B\left(\frac{13}{6},\frac{2}{3}\right)\left(\frac{g_{\mathrm{E}}}{C_{\mathrm{K}}}\right)^{4/9}.$$

For estimation the ratio between integral time scale and Kolmogorov time micro scale $\tau_{\mathrm{K}} = (\nu/\varepsilon)^{1/2}$ we used expression for Reynolds number of turbulence calculated on the base of Taylor micro scale λ (see, for example, [14])

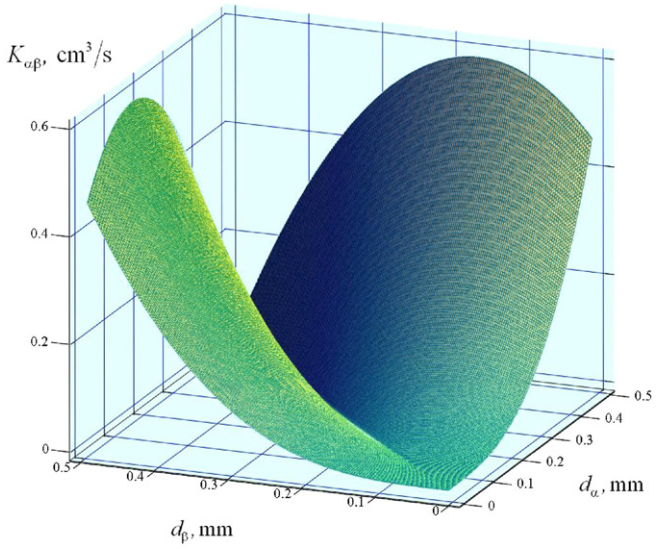

Fig. 20. Gravitational coagulation kernel without turbulence. Droplets diameters for pipe flow.

$$Re_\lambda = \frac{u\lambda}{\nu}, \quad Re_\lambda = \left(\frac{20}{3}\right)^{1/2} \frac{E}{(\nu\varepsilon)^{1/2}}. \tag{A.9}$$

As a result of (A.8) and (A.9) we find

$$\frac{T_E}{\tau_K} = \beta_E \left(\frac{3}{20}\right)^{1/2} Re_\lambda.$$

As an example, for Kolmogorov constant $C_K = 1.67$ [14], we have $\beta_E \approx 0.323$, and $T_E/\tau_K \approx 0.125 Re_\lambda$.

The expressions (A.1), (A.2) and (A.4) enable us to calculate particles response functions for correlations of any gas velocity components. Response function for particles turbulent energy (3) follows after summation (A.2) at $i = j$. For calculation the response function (10) in wave space in spherical coordinates system we carry out the following transformations

$$\begin{aligned} f_\alpha &= \frac{1}{E}\int_0^\infty \widehat{E}^0(k) e^{-\frac{k^2 A_\alpha^2}{2}} dk \frac{1}{\tau_\alpha}\int_0^\infty e^{-\frac{s}{\tau_\alpha}-\omega_k s} ds \frac{1}{2}\int_0^\pi \sin\theta e^{ik\langle W_\alpha\rangle s\cos\theta} d\theta \\ &= \frac{1}{E}\int_0^\infty \widehat{E}^0(k) e^{-\frac{k^2 A_\alpha^2}{2}} dk \frac{1}{\tau_\alpha}\int_0^\infty \frac{\sin(k\langle W_\alpha\rangle s)}{k\langle W_\alpha\rangle s} e^{-\frac{s}{\tau_\alpha}-\omega_k s} ds \\ &= \frac{1}{E}\int_0^\infty \widehat{E}^0(k) e^{-\frac{k^2 A_\alpha^2}{2}} \frac{\operatorname{arctg}\left(\frac{k\tau_\alpha\langle W_\alpha\rangle}{1+\omega_k\tau_\alpha}\right)}{k\tau_\alpha\langle W_\alpha\rangle} dk \end{aligned} \tag{A.10}$$

From expression (A.10) one can see that grows of relative velocity of particles $\langle W_\alpha\rangle$ reduced the response function. Without velocity slip ($\langle W_\alpha\rangle = 0$) from (A10) it is follows

$$f_\alpha = \frac{1}{E}\int_0^\infty \frac{\widehat{E}^0(k)}{1+\omega_k\tau_\alpha} e^{-\frac{k^2 A_\alpha^2}{2}} dk.$$

From last expression one can see that particle inertia also diminishes energy of chaotic motion of dispersed phase.

For discussion the results of comparison DNS data [2,3,19] with theoretical results of our work it is useful obtain spectral presentation in wider region of wave vectors. Distribution of turbulent energy in the area of viscous dissipation is approximated as Pao spectrum [21]

$$\widehat{E}^0_D(k) = C_K \varepsilon^{2/3} k^{-5/3} \exp[-\alpha(k\eta_K)^{4/2}], \tag{A.11}$$

where $\eta_K = (\nu^3/\varepsilon)^{1/4}$ is Kolmogorov space micro scale.

Constant α in (A.11) is found from normalization condition

$$\varepsilon = 2\nu \int_0^\infty k^2 \widehat{E}^0_D(k)\, dk, \quad \alpha = \frac{3}{2} C_K.$$

United turbulent spectra in the all region of turbulent eddies is approximated as follows

$$\widehat{E}^0(k) = \min(E^0_E(k), E^0_D(k)).$$

Fig. 21 illustrates the composition of the branches of turbulent spectra for regions of energy containing eddies and viscous dissipation. Fig. 22 shows dependence of a shape of the spectra on Reynolds number of turbulence Re_λ. One

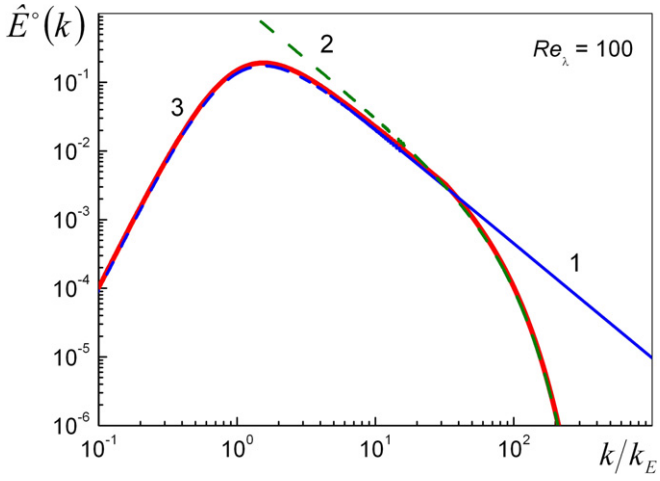

Fig. 21. United turbulent spectra: (1) Carman approximation for energy containing eddies; (2) Pao approximation.

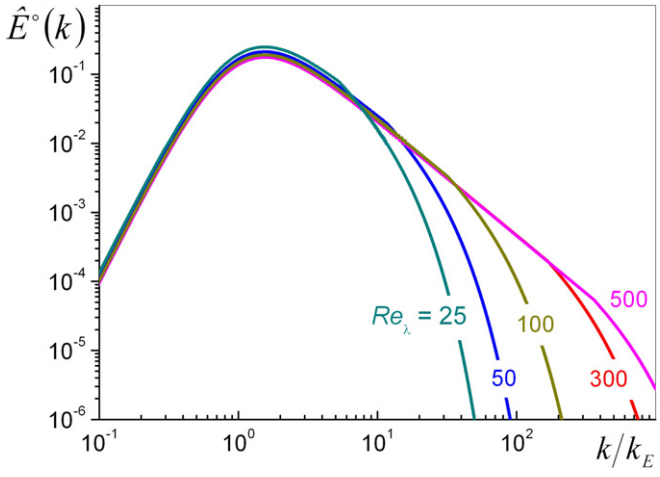

Fig. 22. United turbulent spectra with various Reynolds number of turbulence.

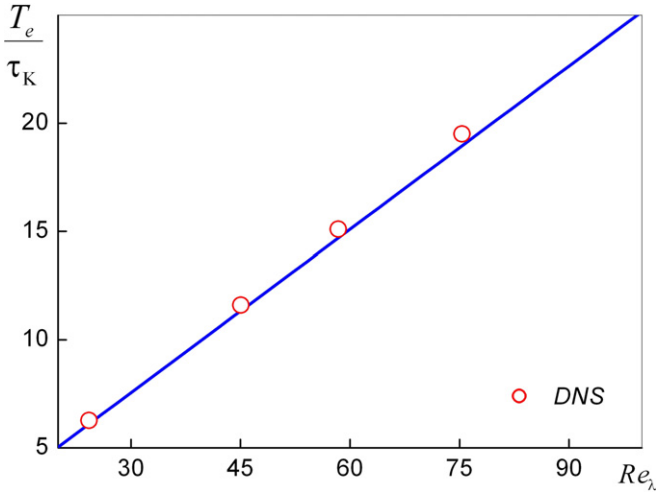

Fig. 23. Ratio integral time scale to Kolmogorov micro scale as a function of turbulence Reynolds number. Line model prediction, points are DNS data [2].

can see that the region of universal energy transfer between turbulent eddies (A.5) is reduced with decreasing Reynolds number of turbulence. Dependence of ratio integral time macro scale at Kolmogorov time micro scale T_E/τ_K is presented in Fig. 23. In Fig. 23 time macro scale is defined for one-dimensional spectra $T_e = 2T_E$ [14].

Appendix B. Averaged value of a random vector module

We present calculation result for averaged module of vector **w** distributed as Gaussian random field. For isotropic case PDF of the random vector is

$$\Phi(\mathbf{w}) = \frac{1}{(2\pi\sigma)^{3/2}}\exp\left(-\frac{\mathbf{w}\cdot\mathbf{w}}{2\sigma}\right) = \prod_{i=1}^{3}\frac{1}{(2\pi\sigma)^{1/2}}\exp\left(-\frac{w_i^2}{2\sigma}\right), \tag{B.1}$$

where $\sigma = \langle w_i^2\rangle$ is average value of square of velocity fluctuations in one direction.

PDF of the random vector module $|w| = \sqrt{\mathbf{w}\cdot\mathbf{w}}$ is obtained after integration over velocity space in spherical coordinates

$$\Phi^0(|w|) = \int_0^{2\pi}\mathrm{d}\varphi\int_0^{\pi}|w|\Phi(\mathbf{w})\sin\theta\,\mathrm{d}\theta = \sqrt{\frac{2}{\pi}}\frac{|w|^2}{\sigma^{3/2}}\mathrm{e}^{-\frac{|w|^2}{2\sigma}}. \tag{B.2}$$

Expression (B.2) is well-known Raleigh distribution with normalization condition

$$\int_0^{\infty}\Phi^0(w)\,\mathrm{d}w = 1.$$

Averaged value of the random vector **w** module is calculated as

$$\langle|w|\rangle = \int_0^{\infty} w\Phi^0(w)\,\mathrm{d}w = \Xi\sigma^{1/2}, \quad \Xi = 2\sqrt{\frac{2}{\pi}}. \tag{B.3}$$

We compare result (B.3) with averaged value of one component of the **w** in positive direction

$$\langle w_+\rangle = \int_0^{\infty}\frac{w}{\sqrt{2\pi\sigma}}\mathrm{e}^{-\frac{w^2}{2\sigma}}\mathrm{d}w = \sqrt{\frac{2}{\pi}}\sigma^{1/2}. \tag{B.4}$$

From expressions (B.3) and (B.4) follows

$$\langle|w|\rangle/\langle w_+\rangle = 2.$$

At the calculation particles response functions arises the transformation of PDF of particle transition

$$G(\mathbf{k},\xi) = \int\frac{1}{(2\pi\Delta^2)^{3/2}}\exp\left(-\frac{|\mathbf{W}\xi-\mathbf{Y}|^2}{2\Delta^2}\right)\exp(\mathrm{i}\mathbf{k}\cdot\mathbf{Y})\,\mathrm{d}\mathbf{Y}. \tag{B.5}$$

In new variable $\mathbf{y} = \mathbf{Y} - \mathbf{W}\xi$ the expression (B.5) has the form

$$G(\mathbf{k},\xi) = \exp(\mathrm{i}\mathbf{k}\cdot\mathbf{W}\xi)\int\frac{1}{(2\pi\Delta^2)^{3/2}}\exp\left(-\frac{\mathbf{y}\cdot\mathbf{y}}{2\Delta^2}+\mathrm{i}\mathbf{k}\cdot\mathbf{y}\right)\mathrm{d}\mathbf{y}.$$

In spherical coordinates the above integral will be as

$$G(\mathbf{k},\xi) = \exp(\mathrm{i}\mathbf{k}\cdot\mathbf{W}\xi)\int_0^{2\pi}\mathrm{d}\varphi\int_0^{\pi}\sin\theta\,\mathrm{d}\theta\int_0^{\infty}\frac{y^2}{(2\pi\Delta^2)^{3/2}} \times\exp\left(-\frac{y^2}{2\Delta^2}+\mathrm{i}ky\cos\theta\right)\mathrm{d}y.$$

After evident calculations we obtain simple expression for PDF of particle transition in the wave space

$$G(\mathbf{k},\xi) = \sqrt{\frac{2}{\pi}}\frac{\exp(\mathrm{i}\mathbf{k}\cdot\mathbf{W}\xi)}{k\Delta^3}\int_0^{\infty}y\sin(ky)\exp\left(-\frac{y^2}{2\Delta^2}\right)\mathrm{d}y = \exp\left(\mathrm{i}\mathbf{k}\cdot\mathbf{W}\xi-\frac{k^2\Delta^2}{2}\right). \tag{B.6}$$

Appendix C. Solution of equation for particles distribution

Form Eq. (44) follows formula for gradient of distribution

$$\frac{\mathrm{d}\langle N_{\alpha\beta}\rangle}{\mathrm{d}r^*} = B\frac{\exp(-\Theta_{\alpha\beta}r^*)}{r^{*2}}, \quad \Theta_{\alpha\beta} = \frac{a_{\alpha\beta}\langle W_{\alpha\beta}\rangle/4}{D_{\alpha\beta}}, \tag{C.1}$$

where $r^* = r/a_{\alpha\beta}$ is dimensionless coordinate; B is integration constant which value will be defined during solution.

Eq. (C.1) leads to following form of $\langle N_{\alpha\beta}\rangle$

$$\langle N_{\alpha\beta}\rangle = A + B\int_1^{r^*}\frac{\mathrm{e}^{-\Theta_{\alpha\beta}t}}{t^2}\,\mathrm{d}t, \tag{C.2}$$

where A is integration constant.

Value of $\langle N_{\alpha\beta}\rangle$ at $r^* = 1$ is $\langle N_{\alpha\beta}\rangle = \langle N_{\alpha\beta}^{(1)}\rangle$. Expression for distribution of particles is finding with the help of (C.2) and boundary condition (45)

$$\langle N_{\alpha\beta}\rangle = \left\langle N^{(1)}_{\alpha\beta}\right\rangle + \frac{\left\langle N^{0}_{\alpha\beta}\right\rangle - \left\langle N^{(1)}_{\alpha\beta}\right\rangle}{E_2(\Theta_{\alpha\beta})}\int_1^{r^*}\frac{\mathrm{e}^{-\Theta_{\alpha\beta}t}}{t^2}\,\mathrm{d}t,$$

$$E_2(x) = \int_1^{\infty}\frac{\mathrm{e}^{-xt}}{t^2}\,\mathrm{d}t, \qquad (C.3)$$

where $E_2(x)$ is integral exponent of second order [18].

Boundary conditions (46) at $r^* = 1$ serves for calculation the boundary value of $\left\langle N^{(1)}_{\alpha\beta}\right\rangle$ and flux of βth particles. Involving (C.1) and (C.3) we write down the following equation

$$\frac{1}{2}\langle W_{\alpha\beta}\rangle\left\langle N^{(1)}_{\alpha\beta}\right\rangle + D_{\alpha\beta}\frac{\left\langle N^{0}_{\alpha\beta}\right\rangle - \left\langle N^{(1)}_{\alpha\beta}\right\rangle}{a_{\alpha\beta}\Theta_{\alpha\beta}E_2(\Theta_{\alpha\beta})} = \frac{1-\chi}{1+\chi}\sqrt{\frac{2}{\pi}\left\langle w^2_{\alpha\beta}\right\rangle}\left\langle N^{(1)}_{\alpha\beta}\right\rangle = J_{\alpha\beta}\langle N^{0}_{\alpha\beta}\rangle. \qquad (C.4)$$

Solution of Eq. (C.4) gives particles distribution at the colliding surface

$$\left\langle N^{(1)}_{\alpha\beta}\right\rangle = \left\langle N^{0}_{\alpha\beta}\right\rangle\left[1 + \Theta_{\alpha\beta}\mathrm{e}^{\Theta_{\alpha\beta}}E_2(\Theta_{\alpha\beta})\left(\frac{\frac{1-\chi}{1+\chi}\sqrt{\frac{2}{\pi}\left\langle w^2_{\alpha\beta}\right\rangle}}{\langle W_{\alpha\beta}\rangle/2} - 1\right)\right]^{-1}.$$

Expression (47) follows from above formula and (C.4).

References

[1] J.R. Fessler, J. Kulick, J.K. Eaton, Preferential concentration of heavy particles in a turbulent channel flow, Phys. Fluids A 6 (1994) 3742–3749.

[2] L.-P. Wang, A.S. Wexler, Y. Zhou, Statistical mechanical description and modeling of turbulent collision of inertial particles, J. Fluid Mech. 415 (2000) 117–153.

[3] Y. Zhou, A.S. Wexler, L.-P. Wang, Modelling turbulent collision of bidisperse inertial particles, J. Fluid Mech. 433 (2001) 77–104.

[4] S. Goto, J.C. Vassilicos, Particle pair diffusion and persistent streamline topology in two-dimensional turbulence, New J. Phys. 6 (2004) 65. Available from: <http://www.njp.org/>.

[5] G. Falkovich, A. Pumir, Intermittent distribution of heavy particles in a turbulent flow, Phys. Fluids. 16 (2004) L47–L50.

[6] C.N. Franklin, P.A. Vaillancourt, M.K. Yau, P. Bartello, Collision rates of cloud droplets in turbulent flow, J. Atmos. Sci. 62 (2005) 2451–2466.

[7] L.P. Wang, A. Orlando, S.E. Kasprzak, W.W. Grabovsky, Theoretical formulation of collision rate and collision efficiency of hydrodynamically interacting cloud droplets in turbulent atmosphere, J. Atmos. Sci. 62 (2005) 2433–2450.

[8] L. Chen, S. Goto, J.C. Vassilicos, Turbulent clustering of stagnation points and inertial particles, J. Fluid Mech. 553 (2006) 143–154.

[9] J. Bec, L.L. Biferale, G. Boffetta, et al., Acceleration statistics of heavy particles in turbulence, J. Fluid Mech. 550 (2006) 349–358.

[10] N. Riemer, A.S. Wexler, Droplets and drops by turbulent coagulation, J. Atmos. Sci. 62 (2005) 1962–1975.

[11] I.V. Derevich, Statistical modeling of mass transfer in turbulent two-phase dispersed flows – 1. Model development, Int. J. Heat Mass Transfer 43 (2000) 3709–3723.

[12] L.I. Zaichik, V.M. Alipchenkov, Pair dispersion and preferential concentration of particles in isotropic turbulence, Phys. Fluids 15 (2003) 1776–1787.

[13] I.V. Derevich, Statistical modeling of particles relative motion in a turbulent gas flow, Int. J. Heat Mass Transfer 49 (2006) 4290–4304.

[14] A.S. Monin, A.M. Yaglom, Statistical Hydromechanics, Part. 2, Nauka, Moscow, 1967, in Russian.

[15] S. Corrsin, Estimation of the relations between Eulerian and Lagrangian scales in large Reynolds number turbulence, J. Atmos. Sci. 20 (1963) 115–121.

[16] M.R. Wells, D.E. Stock, The effect of crossing trajectories on the dispersion of particles in turbulent flow, J. Fluid Mech. 136 (1983) 31–62.

[17] T. Koga, Introduction to Kinetic Theory Stochastic Processes in Gaseous Systems, Pergamon Press, Oxford, 1970.

[18] M. Abramowitz, I.A. Stegun (Eds.), Handbook of Mathematical Functions with Formulas, Graphs and Mathematical Tables, National Bureau of Standards, 1964.

[19] Y. Zhou, A.S. Wexler, L.-P. Wang, On the collision rate of small of particles in isotropic turbulence. II. Finite inertial case, Phys. Fluids 10 (1998) 1206–1216.

[20] H. Siebert, K. Lehmann, M. Wendisch, Observations of small-scale turbulence and energy dissipation rates in the cloudy boundary layer, J. Atmos. Sci. 63 (2006) 1451–1466.

[21] Y.H. Pao, Structure of turbulent velocity and scalar fields at large wave numbers, Phys. Fluids. 8 (1965) 1063–1075.